# Cooperation between Fukushima Prefecture and the IAEA

## In the Area of Radiation Monitoring, Remediation and Waste Management, Following the Fukushima Daiichi Nuclear Power Plant Accident

## (Fukushima Prefecture Initiative Projects)

# INTERIM REPORT

# (2013–2015)

## 【Detailed version】

## (Temporary translation)

## 2016

## Fukushima Prefecture

# Contents

## Introduction

Severe damage was caused by the Tohoku Earthquake that struck on March 11, 2011 and the accompanying accident at the Fukushima Daiichi Nuclear Power Plant operated by the Tokyo Electric Power Company. Restoring the environment after this unprecedented nuclear disaster and creating an environment in which residents of Fukushima Prefecture can live with peace of mind well into the future have become pressing challenges.

It is critical to gather the wisdom of the world and to work to overcome these challenges, and Fukushima Prefecture thus decided to collaborate with the International Atomic Energy Agency (IAEA), which has advanced knowledge in fields concerning nuclear technology. A memorandum of cooperation between Fukushima Prefecture and the IAEA was signed in December 2012.

According to this memorandum, practical arrangements in the fields of decontamination and radiation monitoring between Fukushima Prefecture and the IAEA were signed on the same date. (Projects based on these arrangements are referred to as FCPs.)

Following this, additional arrangements were signed for five projects (referred to below as FIPs) proposed by Fukushima Prefecture in April and October 2013 as a new framework with which to receive support from the IAEA for projects implemented by Fukushima Prefecture.

The five FIPs are the projects and activities listed below.

1) Survey of radionuclide movement in rivers and lakes
2) Survey of radionuclide movement with wildlife
3) Project for studying decontamination technology for rivers and lakes
4) Development of environmental mapping technology using GPS walking surveys
5) Project for the study of promoting the proper treatment of waste containing radioactive materials at municipal solid waste incinerators

FIPs began in 2013, the year in which the practical arrangements were signed, and it was decided to publish this interim report because 3 years have passed since.

Fukushima Prefecture has received various forms of support from the IAEA over the 3 years, the major contents of which are described below.

## Contents of major support received from the IAEA

1) Survey of radionuclide movement in rivers and lakes

- Provision of a TODAM (Time-dependent, One-directional, Degradation and Migrational) model, which is a numerical simulation code of contaminant migration in a river network, for the quantitative estimation of radionuclides deposited in rivers.
- Technical guidance on the selection of monitoring points and monitoring items, and an indication of the importance of continuous monitoring at each monitoring point, based on previous studies for Chernobyl and Mayak.
- Regarding monitoring data obtained by Fukushima Prefecture, advice that measuring Kd values and ion concentrations (especially $K^+$ and $NH_4^+$) in river water at each monitoring point is important for the use of numerical models such as the TODAM model.
- Advice on the effectiveness of combining monitoring and models and adding small lakes and marshes as subjects of research in advancing future research on the dynamics of radioactive substances in rivers.

2) Survey of radionuclide movement with wildlife

- Provision of foreign literature describing the relationship between wild animals and radionuclides, such as the state of radiocaesium in the muscle tissue of wild animals including boars and deer in various regions following the Chernobyl nuclear disaster and changes in radiocaesium levels in the bodies of birds, such as the American gallinule and American wood duck, at the Savannah River Ecology Laboratory.
- Provision of information about the latest scientific results concerning the bioaccumulation of radiocaesium from experts investigating the relationship between wild animals and radioactive substances.
- Advice on the discussion of study results and data analysis methods, such as the potential that mushrooms are the cause of a high radiocaesium concentration in boars of Fukushima Prefecture, arising from the fact that mushrooms (deer truffles) were found to be the cause of a high radiocaesium concentration in the muscle tissue of European boars.

3) Project for studying decontamination technology for rivers and lakes

- Provision of information concerning the environmental dynamics of radioactive substances in rivers, lakes, and marshes of various countries.
- Provision of case studies of environmental remediation measures, such as the decontamination of radioactive substances in rivers, lakes, and marshes of various countries, including countermeasures for the inflow of high concentrations of radioactive

substances to the Pripyat River and measures for suppressing the inflow of radioactive substances to the Kiev Reservoir.

・Advice on the effective implementation of verification tests targeting riverbeds, including the necessity of survey items, survey points, and advance simulations for studies confirming reduced effects of air dose rates and the necessity of survey items (e.g., the size distribution of particles in suspended phases) and weeding test sites when evaluating recontamination.

・Regarding studies of effective radioactive-substance countermeasures targeting river parks, advice to reference past flooding records when selecting survey sites and advice that the dredging and construction of embankments, as well as grit chambers in upstream basins, are effective at sites where there is a concern of recontamination.

4) Development of environmental mapping technology using GPS walking surveys

・Provision of information about efforts made by institutions such as the United States Environmental Protection Agency and Lawrence Berkeley National Laboratory regarding local radiation dose mapping.

・Advice that inverse-distance weighting (IDW) is more appropriate than Kriging as a means of interpolation for walking surveys using the GIS, and that considerations must be made for the shielding effect of buildings and the like.

・Advice to judge measurement conditions of walking surveys by the situation at each measurement point, as it is not always necessary to set uniform measuring conditions.

5) Project for the study of promoting the proper treatment of waste containing radioactive materials at municipal solid-waste incinerators

・Provision of information on treatment methods employed in other countries for fly ash, treatment methods employed in other countries for low-level radioactive waste (i.e., incineration, melting treatment of metal, and plasma melting), and instruments for measuring the concentrations of radioactive substances in waste.

・Technical advice about the incineration of general waste, such as the necessity of studies conducted from the perspective of the caesium balance of payments, the importance of the comparative analysis of actual verification test data and model analysis results, and the necessity of identifying test conditions and assessing waste quality.

・Advice about the importance of countermeasures to the generation of hydrogen fluoride in the mixed incineration of bag filters (made from Teflon).

・Advice on the necessity of checking the safety (e.g. exposure protection and management) of facility workers.

In this manner, Fukushima Prefecture has implemented FIPs with support from the IAEA. The interim report including results of FIPs is provided as follows.

＜This document is issued under the authority and responsibility of the Fukushima Prefecture. ＞

# 1. FIP1: Survey of radionuclide movement in rivers and lakes


## Summary

It is important to provide information necessary for the safe use of river water in the area contaminated by radionuclides. We conducted a survey of rivers flowing through Fukushima Prefecture with the purpose of understanding the dynamics of radionuclides in rivers and verifying dynamics forecasting with numerical models.

To forecast radionuclide dynamics with models, we established data collection necessary for application of the TODAM model to the Hirose River and a monitoring network necessary for verification of dynamics forecasting. Additionally, we conducted a dynamics survey of suspended state radiocaesium adsorbed on small particles that flow downstream in the Abukuma River System and major rivers in the Hamadori area. As a result, we observed a decreasing trend in particulate radiocaesium and regional variation in the rate of decreasing radiocaesium concentration depending on land use in the basin.


## 1.1. Introduction

River water is widely used for tap water and agricultural water. Owing to the accident at the Fukushima Daiichi Nuclear Power Plant in 2011, Fukushima Prefecture was widely contaminated by radionuclides. Because basins have been contaminated, it is an important challenge for us to understand the dynamics of radionuclides in rivers and to provide information necessary for the safe use of river water. It is also important to grasp the dynamics of radiocaesium in the following two forms. In the case that radiocaesium is adsorbed onto suspended sediments (i.e., the so-called particulate form of radiocaesium), the effect of redeposition during floods on the air dose is a concern. Meanwhile, it is also necessary to consider migration through agricultural crops and the ecosystem when radiocaesium flows in a dissolved form (Figure 1). We therefore studied rivers flowing through Fukushima Prefecture to clarify the dynamics of radionuclides in

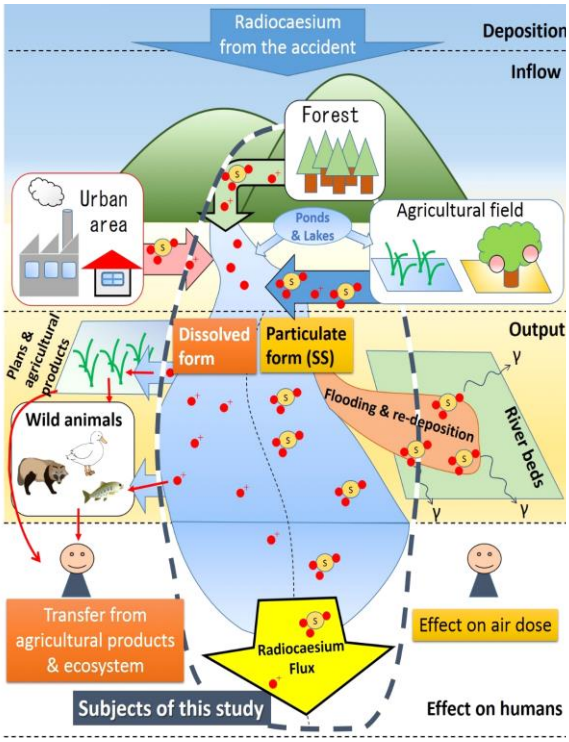


*Figure 1: Schematic view of radiocaesium dynamics in river basins*

rivers, with the additional purpose of verifying the forecasting of dynamics of radionuclides with numerical models using the monitoring data obtained.

## 1.2. Methods

(1) Survey in the Hirose River Basin

We conducted a 3-year study of the Hirose River and its tributaries beginning in 2013. Figure 2(a) shows the inventory of caesium-137 on July 2, 2011 in the basin. Near the basin boundaries on the southeast side, the area marked red has been checked, and there is a high amount of radiocaesium deposition near the basin boundaries on the southeast side and in the Nuno River Basin and Oguni River Basin, which are basins of two tributaries of the Hirose River (Table 1).

*Table 1: Relationship between the catchment area and average caesium-137 inventory for the Hirose River, Nuno River, and Oguni River*

| | Catchment area ($km^2$) | Average Cs-137 inventory ($kBq\ m^{-2}$) |
|---|---|---|
| Hirose River | 269 | 227 |
| Nuno River | 18 | 343 |
| Oguni River | 41 | 345 |

We collected samples at various sites in Figure 2(a); the primary monitored items are given in Table 2. Among the monitored items, the radiocaesium concentration in water samples was measured after the following pretreatment. Raw water was filtered using a membrane filter with a pore size of 0.45 μm. Ten-liter specimens of raw water and filtrate were passed at a rate of 20 mL/minute through columns (inner diameter: 5 cm, height: 40 cm) filled with 40 g each of anion exchange resin and cation exchange resin. After passing the specimens through the columns, the resin was dried at 105 °C, sealed in specialized containers (U-8), and used as specimens for measurement. The concentration of radiocaesium was measured with methods conforming to *γ-ray Spectrometry using a Germanium Semiconductor Detector* (MEXT, 1992).

*Table 2: Major observation items*

| | | |
|---|---|---|
| Survey of river shape | | Cross section diagram, Latitude, Longitude, Elevation, Vegetation information |
| Measurement of radiation dose rate | | Radiation dose rate (1 m, 1 cm) |
| Consecutive observations | | Water level, Turbidity |
| Normal stage of water flow | Monitoring | Discharge, Velocity |
| | Water sample | Turbidity, Suspended solids (SS), pH, Oxidation-reduction potential (Eh), Radioactive concentrations of caesium (Cs-134, Cs-137), Concentrations of $Ca^{2+}$ and $NH_4^+$ |
| | Soil sample | Particle size distribution, Mineral composition, Radioactive concentrations of caesium (Cs-134, Cs-137) |
| During flooding | Monitoring | Discharge, Velocity |
| | Water Sample | Radioactive concentrations of caesium (Cs-134, Cs-137), Concentrations of $Ca^{2+}$ and $NH_4^+$ |

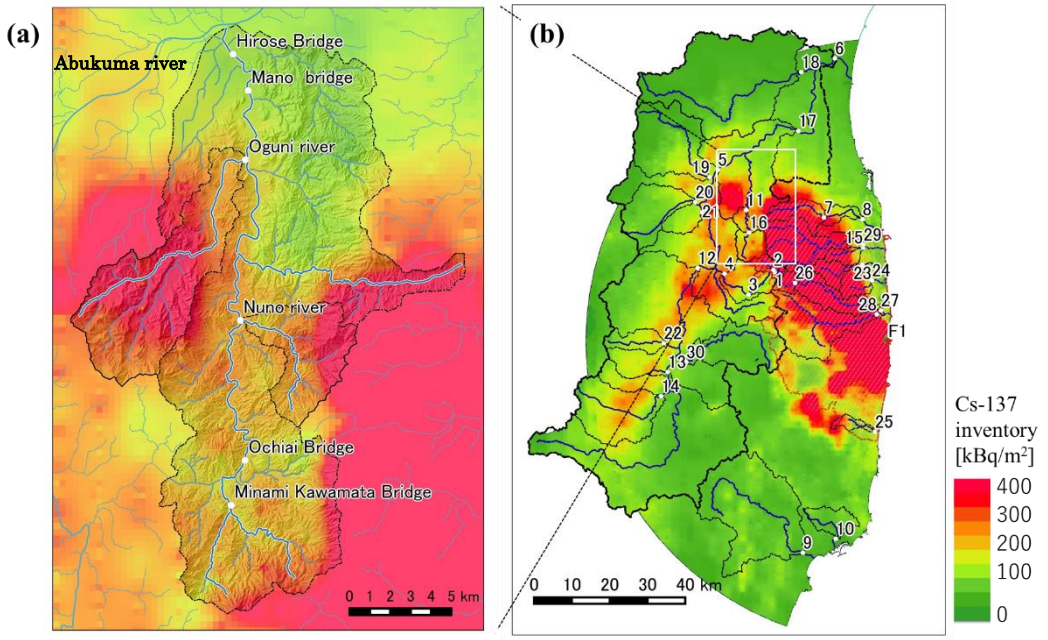


*Figure 2: Map of the locations of monitoring sites and caesium-137 inventory on July 2, 2011*

*(a) Hirose River Basin. (b) Area subject to a wide-area survey. Numbers in the figure correspond to the site numbers in Table 3.*

** Source: Results of the Third Airborne Monitoring Survey conducted by MEXT (2011) http://radioactivity.nsr.go.jp/en/contents/5000/4182/24/1304797_0708e.pdf*
*However, (b) is complemented using results of airborne monitoring by prefecture (http://emdb.jaea.go.jp/emdb/en/portals/b224/) and Results of Radioactive Caesium Deposition of the First Unmanned Helicopter Monitoring within the 3 km Radius from the Fukushima Dai-ichi NPP (http://emdb.jaea.go.jp/emdb/en/portals/b225/) for areas outside the survey range of the Third Airborne Monitoring Survey.*

(2) Wide-area survey on the riverine transport of radiocaesium

Since 2015, we have conducted multi-point river surveys of the Abukuma River System and eight river systems in the Hamadori area. Figure 2(b) shows a map of the locations of monitoring sites and the caesium-137 inventory. Whereas the survey in the Hirose River was a detailed survey of a single basin, the purpose of this wide-area survey is to understand the effect of features of the basins on the long-term changes of radiocaesium dynamics by continuing surveys in multiple rivers employing the same methods. This survey inherited a survey conducted by the University of Tsukuba and commissioned by MEXT and the Nuclear Regulation Authority (NRA) until the end of the 2014 fiscal year. In this report, we introduce results together with past monitoring data. At each monitoring point, we set up a suspended sediment sampler to collect suspended sediment samples, a turbidity meter to measure the turbidity of river water, and a water level meter to measure water depth. At some sites, we use water level data recorded by Fukushima Prefecture and the Ministry of Land, Infrastructure, Transport, and Tourism instead of making measurements with water level meters. We collected suspended sediment trapped in the sediment samplers once every month or once every few months. After an absolute drying treatment at 110 °C for 24 hours, we measured the concentration of particulate caesium-134 and caesium-137 using germanium detectors. The suspended sediment concentration [g/L] and flow rate [$m^3$/s] were calculated using conversion formulas created for turbidity and water level respectively (acquiring data every 10 minutes for each).

*Table 3: Catchment area and average caesium-137 inventory in the wide-area river survey*

| Site No. | Point Name | River System | River Name | Catchment Area [km$^2$] | Average caesium-137 Inventory [kBq m$^{-2}$] |
|---|---|---|---|---|---|
| 1 | Mizusakai River | Abukuma River | Kuchibuto River | 8 | 587 |
| 2 | Kuchibuto River Upstream | Abukuma River | Kuchibuto River | 21 | 408 |
| 3 | Kuchibuto River Midstream | Abukuma River | Kuchibuto River | 63 | 304 |
| 4 | Kuchibuto River Downstream | Abukuma River | Kuchibuto River | 135 | 248 |
| 5 | Fushiguro | Abukuma River | Abukuma River | 3645 | 102 |
| 6 | Iwanuma | Abukuma River | Abukuma River | 5313 | 96 |
| 7 | Mano | Mano River | Mano River | 76 | 521 |
| 8 | Ojimadazeki | Mano River | Mano River | 111 | 418 |
| 9 | Matsubara | Same River | Same River | 871 | 46 |
| 10 | Onahama | Fujiwara River | Fujiwara River | 70 | 45 |
| 11 | Tsukidate | Abukuma River | Hirose River | 84 | 222 |
| 12 | Nihonmatsu | Abukuma River | Abukuma River | 2380 | 88 |
| 13 | Miyoda | Abukuma River | Abukuma River | 1287 | 77 |
| 14 | Nishikawa | Abukuma River | Shakado River | 289 | 137 |
| 15 | Kitamachi | Niida River | Mizunashi River | 36 | 537 |
| 16 | Kawamata | Abukuma River | Hirose River | 57 | 226 |
| 17 | Marumori | Abukuma River | Abukuma River | 4124 | 113 |
| 18 | Funaoka Ohashi | Abukuma River | Shiraishi River | 775 | 27 |
| 19 | Senoue | Abukuma River | Surikami River | 313 | 51 |
| 20 | Yagita | Abukuma River | Ara River | 185 | 63 |
| 21 | Kuroiwa | Abukuma River | Abukuma River | 2921 | 109 |
| 22 | Tomita | Abukuma River | Ouse River | 73 | 117 |
| 23 | Ota | Ota River | Ota River | 50 | 1638 |
| 24 | Odaka | Odaka River | Odaka River | 50 | 750 |
| 25 | Asami | Asami River | Asami River | 26 | 197 |
| 26 | Tsushima | Ukedo River | Ukedo River | 25 | 813 |
| 27 | Ukedo | Ukedo River | Ukedo River | 153 | 2329 |
| 28 | Takase | Ukedo River | Takase River | 264 | 696 |
| 29 | Haramachi | Niida River | Niida River | 200 | 858 |
| 30 | Akanuma | Abukuma River | Otakine River | 243 | 57 |
| 31 | Watari | Abukuma River | Abukuma River | 5313 | 96 |

*The Watari Point (31) is on the bank opposite the Iwanuma Point (6), and was setup as a backup.

## 1.3. Results

(1) Survey in the Hirose River Basin

Figure 3 shows cross-sectional views of the riverbed and photographs taken at the Ochiai Bridge and Mano Bridge monitoring sites on the Hirose River. The two sites are separated by approximately 24 km. Although the water depth does not vary appreciably between the two points, the river width including the flood channel at Mano Bridge is approximately twice the width at Ochiai Bridge, and much sand and gravel is carried by the river and deposited on the flood plain at Mano Bridge.

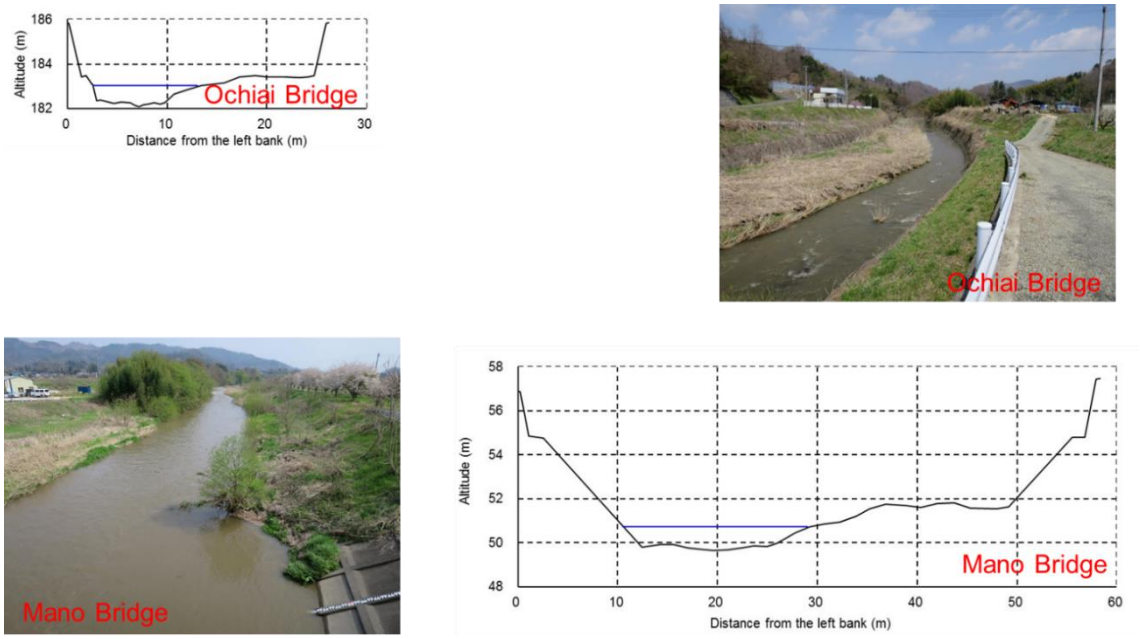


*Figure 3: Photographs and cross-sections of sites in the Hirose River Basin*

Figure 4 shows the changes in precipitation, daily flux of caesium-137, suspended solids (SS) concentration, and discharge monitored in the Hirose River (Ochiai Bridge) from September to December 2014. Heavy rains were observed when two typhoons passed Japan in October 2014. These rains increased the river flow rate considerably, and the concentration of SS in river water increased simultaneously. The daily flux of caesium-137 was calculated from the SS flux and caesium-137 concentration in river water at this time. As a result, the caesium-137 daily flux was high when the river discharge increased because of the two typhoons.

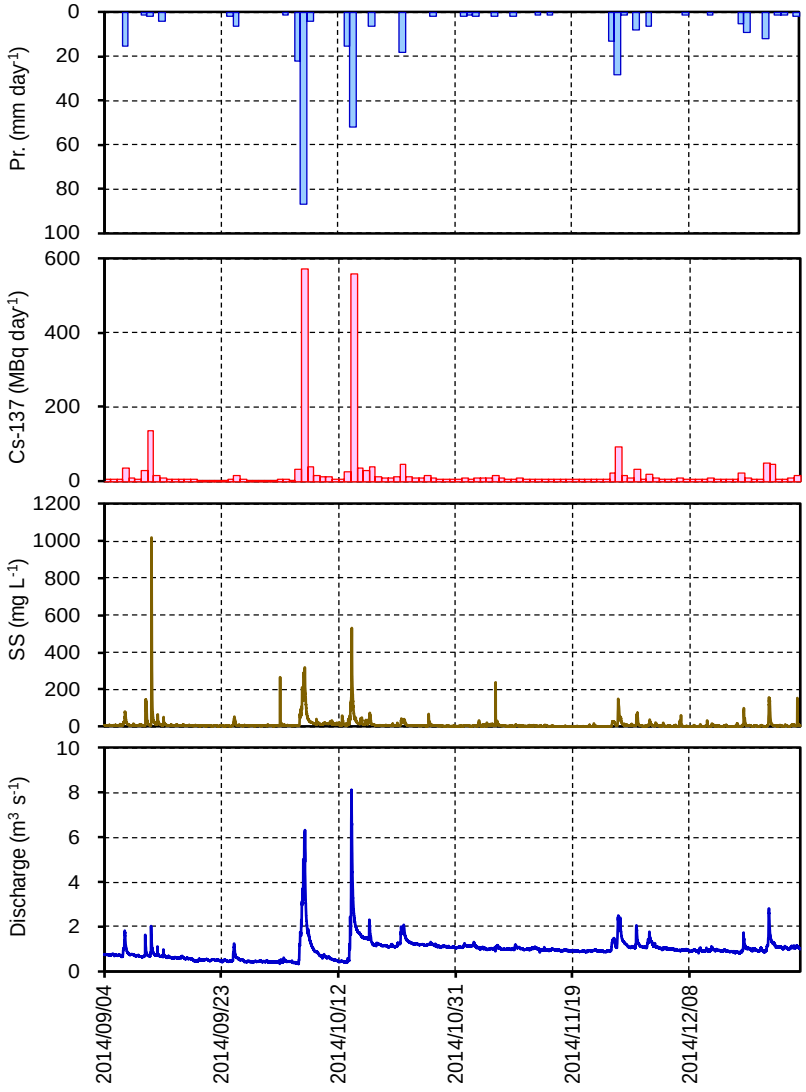


*Figure 4: Changes in precipitation, caesium-137 daily flux, SS concentration, and discharge at Ochiai Bridge on the Hirose River*

Figure 5 shows results for the particulate caesium-137 concentration at monitoring sites in the Hirose River Basin. The figure presents results of collection and measurement at parts of each monitoring site flowing at low-and high speed during the normal stage of water flow on November 9, 2013, and the results of collection and measurement during a flood on July 23, 2013. In samples taken during the normal stage of water flow, the caesium-137 concentration was low in both low- and high-velocity zones, falling below minimum detection values (0.05 Bq $L^{-1}$) at some points. The concentration remained low at both monitoring sites on the Nuno River and Oguni River (Table 1), which have much caesium-137 deposited upstream. However, the caesium-137 concentration was high at all sites in the Hirose River Basin during floods.

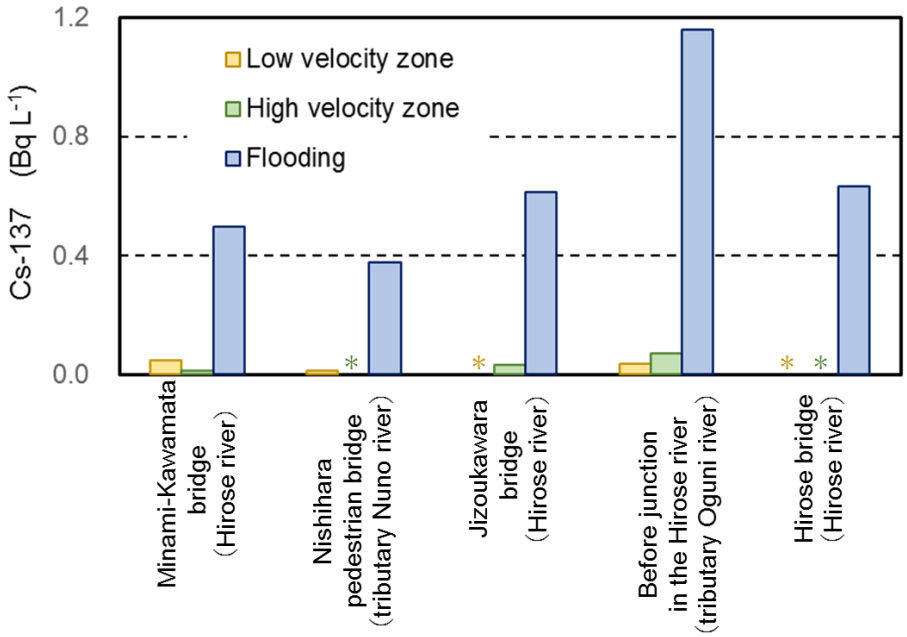


*Figure 5: Concentrations of particulate caesium-137 in the Hirose River Basin*

** below detection limit (0.05 Bq $L^{-1}$)*

Figure 6 shows the measurement results for the caesium-137 concentration in riverbed soil at various monitoring points in the Hirose River Basin. A comparison of results for 2013 and 2014 reveals there was no clear change in trends in the caesium-137 concentration in riverbed soil. The caesium-137 concentration was higher in both low- and high-velocity zones further downstream, with low-velocity zones tending to have a higher concentration than high-velocity zones. The caesium-137 concentration was higher in riverbed soil of the Nuno River and Oguni River, and in riverbed soil of the Hirose River after these two rivers merge.

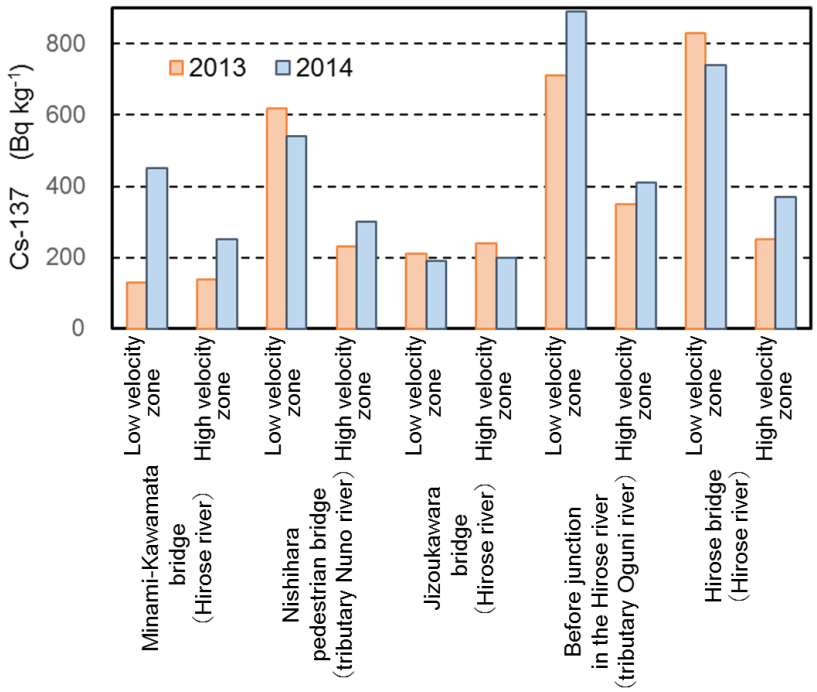


*Figure 6: Caesium-137 concentration in riverbed soil of the Hirose River Basin*

To forecast radionuclide dynamics in the Hirose River with numerical models, we collected necessary data and established a monitoring network for verification of dynamics forecasting in the Hirose River Basin. In the 2015 fiscal year, Professor Yasuo Onishi of Washington State University provided us with the TODAM model to use for model computation in the case of the Hirose River, and advice on methods of operation. It will be necessary to conduct a model computation of radionuclide dynamics in the Hirose River Basin by implementing continuous river monitoring and using the results obtained.

(2) Wide-area survey

In the wide-area survey, sites 1–6 are long-term monitoring sites that have been subject to continuous monitoring since June 2011. Changes over time in the particulate caesium-137 concentration [Bq/kg] at these sites are shown in Figure 7. While high values exceeding 10,000 Bq/kg were observed at all sites immediately after the accident, values have tended to decrease to less than one-tenth of the initial concentrations over 5 years. The rate of decline was highest in the first year after the accident, and has decreased from the second year onwards.

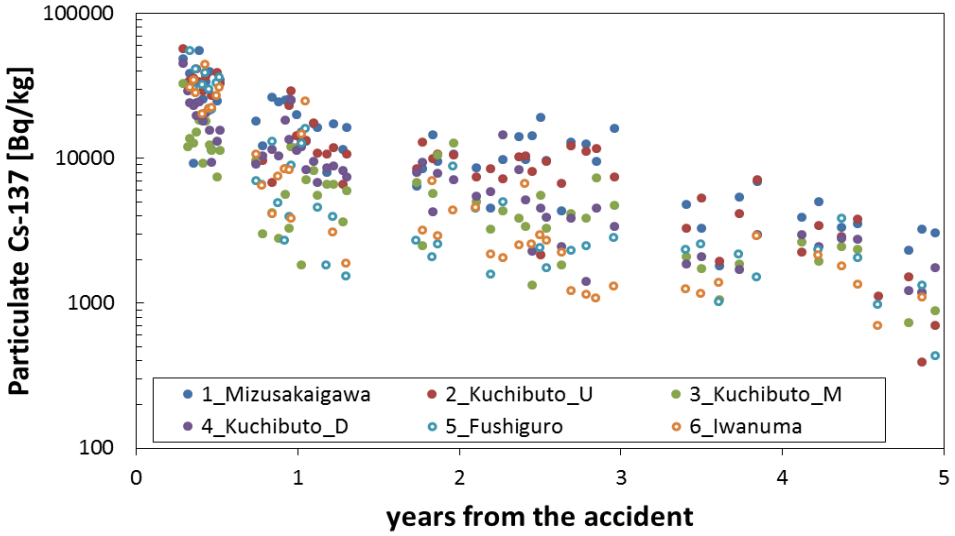


*Figure 7: Temporal change in the particulate caesium-137 concentration at six long-term monitoring sites*

The transition of monthly particulate caesium-137 flux until August 2015 at the same six long-term monitoring sites is shown in Figure 8. Unlike the case for the caesium-137 concentration, there was no clear declining trend for the caesium-137 flux. This is because the fluctuation ranges of the flow rate and suspended sediment concentration depending on the presence of floods were far larger than the range of the decrease (one order of magnitude) of the radiocaesium concentration. In addition, the ratio of the integrated value of the particulate caesium-137 flux relative to the caesium-137 inventory at each point in the basin (i.e., caesium-137 inventory multiplied by the catchment area) was 2.7% to 3.4% at two points on the Abukuma main channel and 0.7% to 1.4% at four points on tributaries of the main channel (Figure 9).

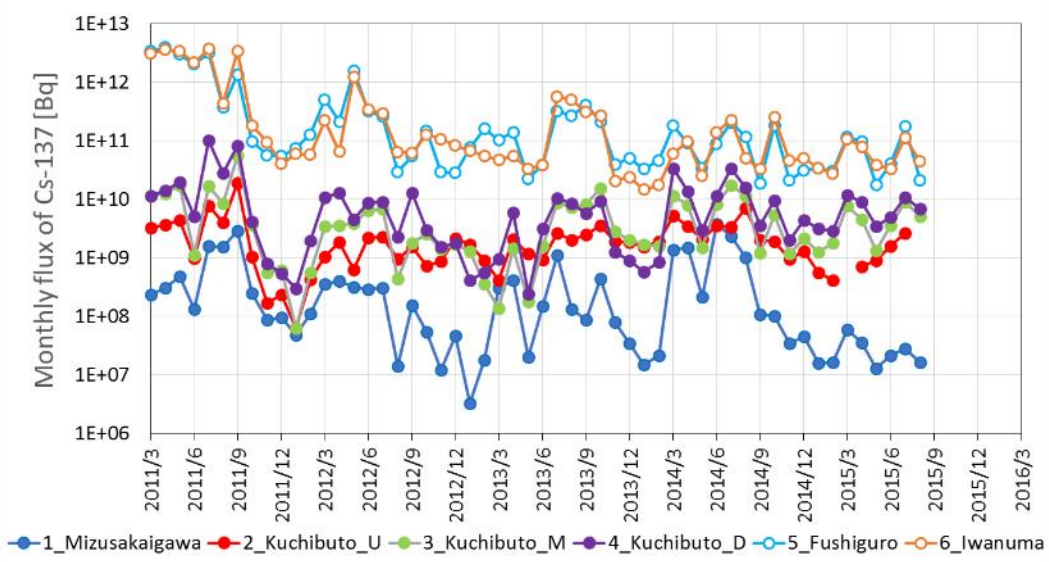


*Figure 8: Transition of particulate caesium-137 flux until August 2015 at six long-term monitoring sites*

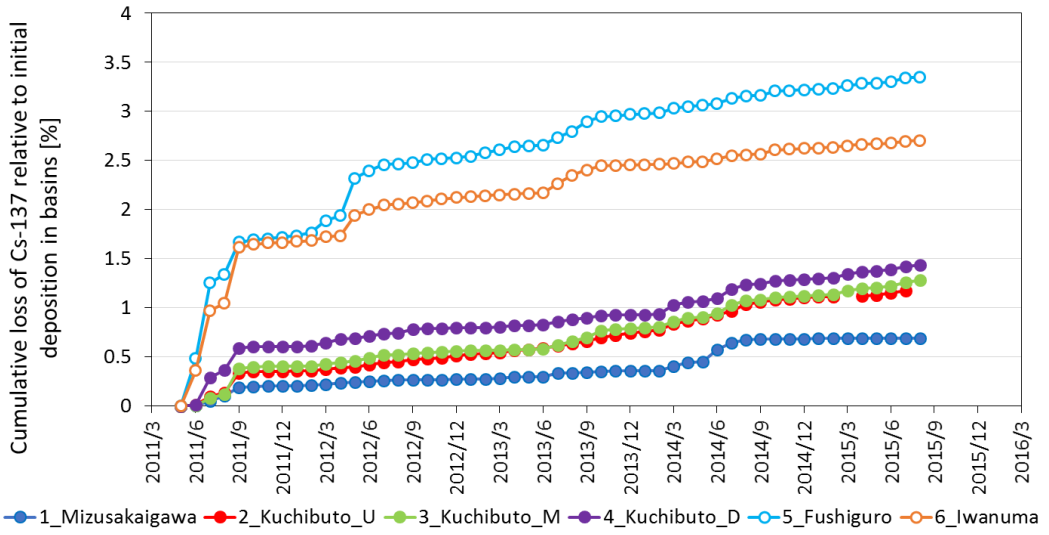


*Figure 9: Cumulative loss of caesium-137 relative to initial deposition in basins after June 2011 at six long-term monitoring sites*

The NRA (2015) stated that the difference in the declining rate of the caesium-137 concentration was due to the variation in land use between monitoring sites (source: *Aggregation of data on the distribution and development of migration model for radionuclides due to the Tokyo Electric Power Company Fukushima Daiichi Nuclear Power Plant accident in fiscal year 2014. Part 2: Survey on radiocaesium transport in river systems*, http://radioactivity.nsr.go.jp/ja/list/560/list-1.html). Caesium-137 concentrations per initial deposition in the basin [Bq $kg^{-1}$/Bq $m^{-2}$] at sites 1–16 from August 2011 to the end of 2014, which can be obtained as the caesium-137 concentration divided by the average caesium-137

inventory for each basin, were approximated using the exponential function ($y = a\ \exp(-kt)$) (Figure 10). The rate of decline $k$ [year$^{-1}$] is plotted with respect to the coverage of land-use types in Figure 11. The value of $k$ increased with the coverage rates of paddy fields, urban areas, and farmland.

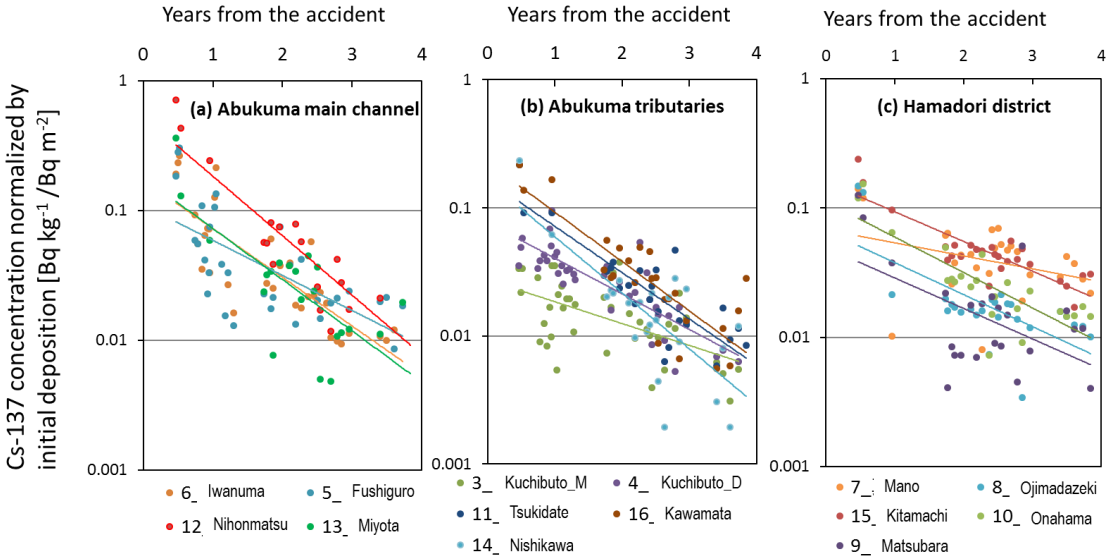


*Figure 10: Caesium-137 concentration per initial deposition in the basin (August 2011 to the end of 2014). There are differences in the rate of decrease depending on the geographic point. (NAR, 2015, partially revised)*

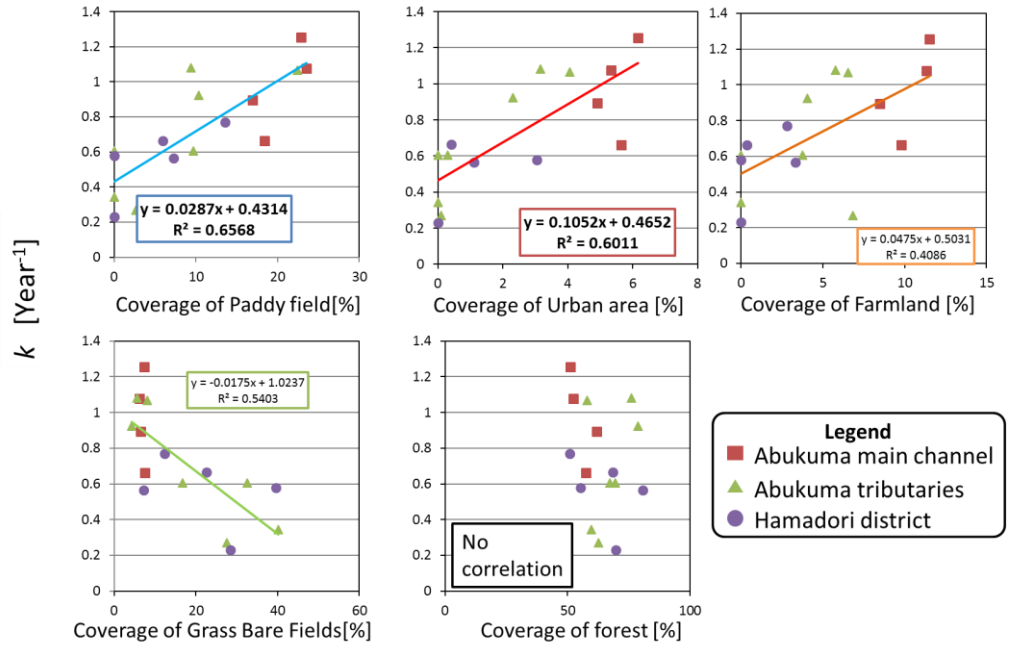


*Figure 11: Rate of decrease in the caesium-137 concentration per initial deposition in basins from August 2011 to the end of 2014 (NAR, 2015, partially revised)*

## 1.4. Conclusion

To forecast radionuclide dynamics in the Hirose River with numerical models, we established a collection of necessary data for application of the TODAM model and a monitoring network necessary for verification of dynamics forecasting in the Hirose River Basin by the 2015 financial year. We also performed a wide-area survey of the Abukuma River System and major rivers in the Hamadori area. The levels of radiocaesium adsorbed by small particles in water continuously declined; the rate of decline was affected by the type of land use in the catchment area.

# 2. FIP2: Survey of radionuclide movement with wildlife

**Summary**

To understand the dynamics of radionuclides in the ecosystem of Fukushima Prefecture, we are studying how radionuclides are assimilated into wild animals, which constitute part of the ecosystem. We measured the concentration of radiocaesium in the bodies and food of wild animals, and analyzed the temporal change and differences among species.

Furthermore, having studied the home range of wild animals because the behavior of wild animals is closely related to the dynamics of radionuclides in the ecosystem, we found that the home range of wild boars inside the evacuation zone tended to be larger than that outside the evacuation zone.

## 2.1. Purpose

The accident at the Fukushima Daiichi Nuclear Power Station caused wide ranging environmental pollution in the form of radioactive substances. Wild animals living in the natural environment assimilate radioactive substances into their bodies by, for example, eating food. As a result, radionuclides have been found in the bodies of many wild animals.

In Fukushima Prefecture, we have monitored radionuclides in the muscles of game wild animals since immediately after the accident in 2011, to ensure the safety and security of the living environment for hunters and prefectural residents. In the measurement of artificial gamma-ray emitting nuclides contained in muscle, radionuclides other than caesium-134 and caesium-137 have been below the detection limit. However, because there is little knowledge about the movement of radiocaesium from the ecosystem into wild animals, we began a study to understand the dynamics of radiocaesium in the ecosystem. It has been speculated that the behavior of wild animals is closely related to the movement of radiocaesium into wild animals. However, much remains unknown about the behavior of wild animals, and research on the behavior of wild animals in areas uninhabited by humans due to evacuation orders is particularly scarce. We thus studied the behavior of wild animals.

## 2.2. Implementation Details

Boars were chosen as the main wild animal species for this study, as they are distributed broadly throughout Fukushima Prefecture, and the caesium-137 concentration in wild boar did not have an obvious downward trend with time in studies of the accident at the Chernobyl Nuclear Power Plant. We will eventually expand the study to other wild animal species.

(1) Dynamics of radionuclides in wild animals

a) Measurement of the concentration of gamma-ray-emitting nuclides in the bodies of wild animals

In the measurement of the radionuclide concentration in the bodies of wild animals, we measured the concentration of gamma-ray-emitting nuclides contained in muscle of animals (mainly boar and black bear, wet weight) that were killed through hunting and pest control following the procedures illustrated in Figure 1. In addition, we measured the concentration of gamma-ray-emitting nuclides in the internal organs of boars using the same procedure to show the distribution of radionuclides in the body.

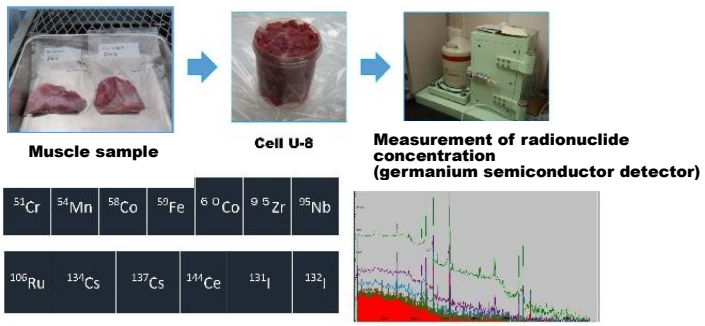


*Figure 1: Measurement of radionuclides in wild animals*

b) Movement of radionuclides into the bodies of wild animals from the environment

We conducted a composition analysis of the stomach contents of boars to show their diet. According to the results of the analysis and the opinions of experts, we sampled the food of boars in the area around the point that they were captured. We then measured the concentration of gamma-ray-emitting nuclides in the food samples.

We also examined the potential that boars consume food that naturally contains a high concentration of gamma-ray-emitting nuclides.

c) Form of radiocaesium contained in stomach contents

The form of radiocaesium is related to the absorption of the radiocaesium from soil into plants. Similarly, we considered the effect of the form of radiocaesium contained in the stomach contents on the absorption of radiocaesium into the bodies of boars.

(2) Survey of the home range of wild animals

We studied the behavior and home range of boars by attaching a GPS data logger (GPS collar, Figure 2) to each boar's body. Using GPS points recorded every 15 minutes by the GPS collar, we investigated the behavior of boars both inside and outside the evacuation area (Figure 3).

*Figure 2: GPS collar*

*Figure 3: Attaching a GPS collar to a boar that was captured with the help of a nuisance animal capture squad and sedated.*

## 2.3. Results

(1) Dynamics of radionuclides in wild animals

a) Measurement of the concentration of gamma-ray-emitting nuclides in the bodies of wild animals

Figure 4 shows the trend of the caesium-137 concentration in boar muscle from May 2011 to December 2015. The figure shows the date the wild boar was captured on the X-axis and the log-transformed caesium-137 concentration on the Y-axis, with black circles giving the measurement of each individual. A bar, error bar, and box show the geometric mean, maximum and minimum values, and the 25% to 75% confidence interval, respectively.

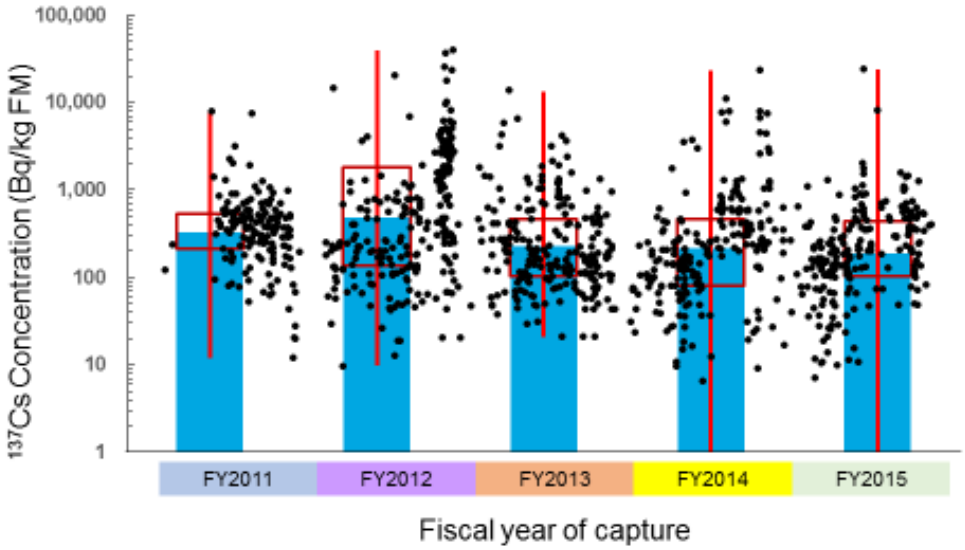


*Figure 4: Results of monitoring the caesium-137 concentration in the muscle of wild boars (fiscal years from May 2011 to December 2015)*

The average caesium-137 concentration appears to have decreased after the 2012 fiscal year. However, the caesium-137 concentration varied appreciably depending on the characteristics of the particular areas where the measurements were taken. For comparison with the case for the boars captured in Fukushima Prefecture, we show the case of Regensburg in southern Germany, where boars were captured and studied following the Chernobyl Nuclear Accident, in Figure 5 (Semizhon et al., 2009). The caesium-137 concentration varied widely but, similar to the case for Fukushima Prefecture, there was no clear downward trend. It is necessary to examine the trend of the caesium-137 concentration in wild boar of Fukushima Prefecture in the future.

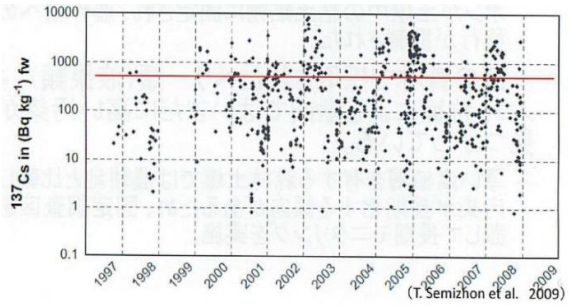


*Figure 5: Temporal trends of caesium-137 in the muscle of boars (Regensberg, Southern Germany)*

Data on the caesium-137 concentration in soil measured by MEXT from 2011 to 2012 are shown in Figure 6. It is possible that the concentration of radiocaesium in boar muscle is related to the concentration of radiocaesium in soil. We have examined this correlation in detail by, for example, setting provisional soil contamination levels.

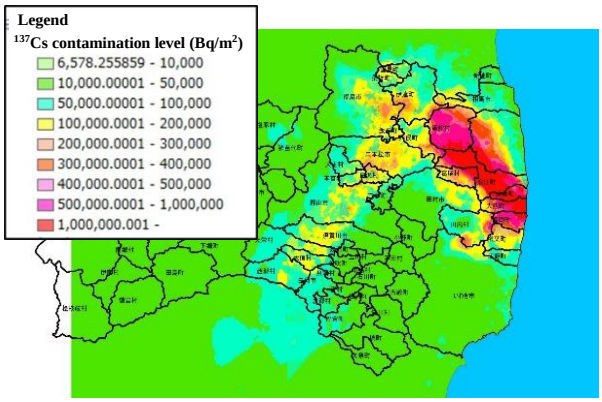


*Figure 6: Caesium-137 soil contamination level (Fukushima Prefecture)*

The caesium-137 concentration in Asian black bear muscle is shown in Figure 7. The concentration appears to have decreased with time, and the fiscal-year average caesium-137 concentration decreased until the 2014 fiscal year.

We thus confirmed that temporal trends of the caesium-137 concentration vary depending on the species of wild animal. A comparison of the caesium-137 concentrations contained in various organs of boars, including the muscle, heart, liver, lung, and kidney, shows that the caesium-137 concentration was highest in muscle and that there was a

certaincorrelation in concentrations between muscles and various organs. There was a small number of samples and greater scrutiny will thus be needed in the future, but we expect this study will contribute to showing the distribution of caesium-137 in the boar body and the radiocaesium concentration in the whole boar body.

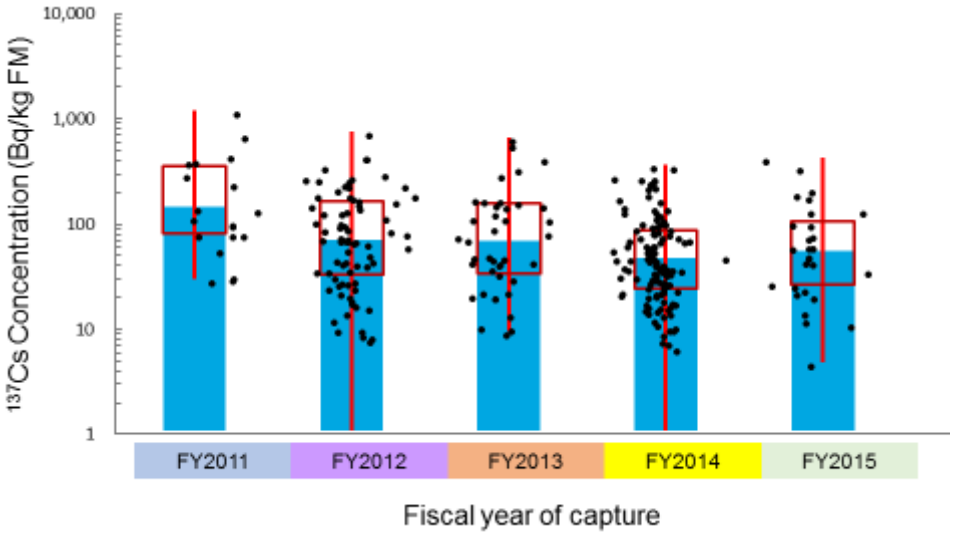


*Figure 7: Results of monitoring the caesium-137 concentration in the muscle of Asian black bear (fiscal years from May 2011 to December 2015)*

b) Movement of radionuclides into the bodies of wild animals from the environment

Having conducted a composition analysis of the stomach contents of boars, we found that the contents can be roughly divided into four categories depending on the season: January to March, April to June, July to September, and October to December. It is believed that the composition of the food eaten by boars changes with the seasons. In any season, vegetable matter was most common food and animal matter accounted for at most a few percent of the food. In the future, we will investigate the seasonal changes in the concentration of radiocaesium in the stomach contents, and the correlation of the concentrations of radiocaesium in the muscles and stomach contents.

*Figure 8: Compositional analysis of stomach contents; stomach contents are sieved and analyzed under a microscope*

In Europe, the cause of the high concentration of radiocaesium in boar muscle was believed to be the fungus tsuchidango (deer truffle). In the composition analysis of stomach contents, we could not find any pieces of fungi. Additionally, we should be able to see a seasonal fluctuation of the caesium-137 concentration if fungi were the cause of the high caesium-137 concentration in the muscle of the boars, but to date, no such trend has been seen in Fukushima Prefecture. We will continue the investigation of the relationship between fungi and the caesium-137 concentration in the bodies of wild boars.

c) Form of radiocaesium contained in stomach contents

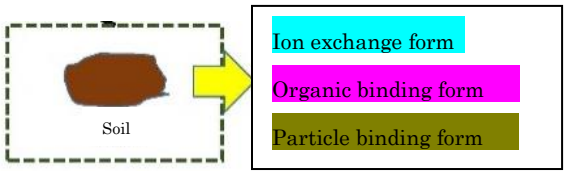


*Figure 9: State of caesium in soil*

Caesium in soil has three forms (Figure 9). The ion exchange form is mainly absorbed by plants while the particle binding form coupled with clay minerals is difficult to absorb. It is thought that boars eat soil together with food when consuming subterranean food, or that they eat soil intentionally to obtain minerals, and there is thus the potential for caesium-137 in soil to be absorbed into the body. We are continuing surveys to show that soil consumption and the form of radiocaesium in the soil are responsible for the caesium-137 concentration in muscle being higher in boars than in other wild animals.

(2) Survey on the home range of wild animals

Although boars have a stable home range like that illustrated in Figure 10, there are no data of details such as the shape, area, and internal structure of the home range. In a survey on the home range of boars, we were able to divide the home range into residential zones with a high point density (areas including nearly 95% of GPS points according to density analysis) and a roaming zone (minimum convex polygon) in which all GPS points were included, as shown in Figure 11. In this case, the analysis shows that the boars had two residential zones, the total area of which was approximately 37 ha, and that the boars had a total home range of 244 ha.

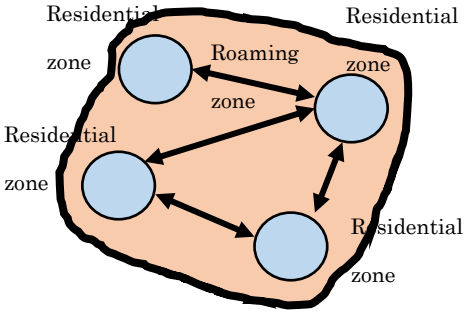


*Figure 10: Structural diagram of a home range*

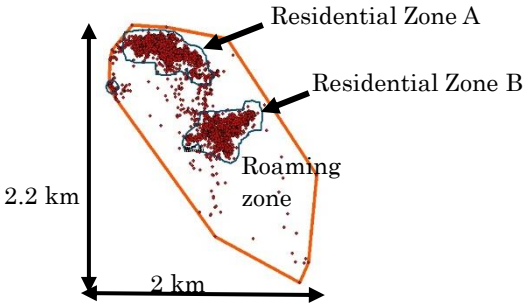


*Figure 11: Structure of the actual home range*

Taking the analysis further, there were areas within residential zones where GPS points were clustered densely, which we have labeled as the residential core (Figure 12). The area of the residential core was very small, being only 3.3 ha in this case.

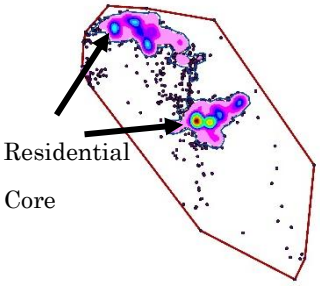


*Figure 12: Residential core*

a) Home range of boars outside the evacuation area

Outside the evacuation area, we surveyed the boar home range in Fukushima City, located in a peri-urban area, and Tazawa in Nihonmatsu Iwashiro District, located in a mountainous area. Results are presented on the same scale in Figure 13 (with a 1 km$^2$ mesh).

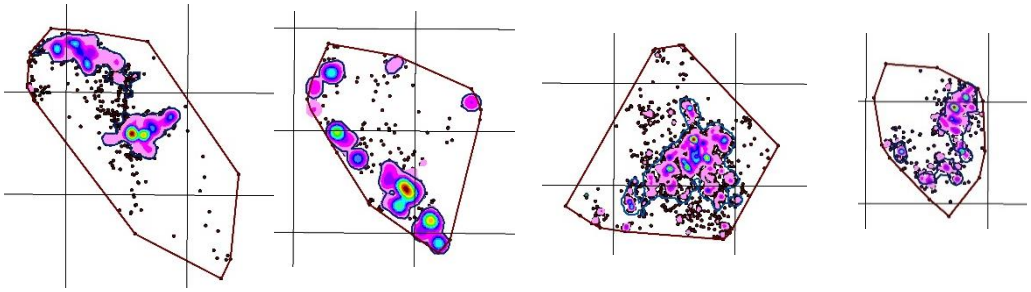

| No. 52, Fukushima City (♂) | No. 58, Fukushima City (♂) | No. 66, Nihonmatsu City (♀) | No. 67, Nihonmatsu City (♀) |
|---|---|---|---|
| Residential zone: 37 ha | Residential zone: 41 ha | Residential zone: 51 ha | Residential zone: 20 ha |
| Home range: 244 ha | Home range: 186 ha | Home range: 207 ha | Home range: 97 ha |

*Figure 13: Size of boar home range outside the evacuation area*

Although individual differences can be seen, the residential zone where the boars spend most of their lives was just 20 to 50 ha. The roaming zone was only 100 to 250 ha, suggesting that boars are the type of animal that settles in one region.

b) Home range of boars inside the evacuation area

To investigate what constitutes the home range of boars when human activity has declined, we surveyed the home range of boars in Tomioka Town, which has been designated an evacuation zone. Figure 14 shows the results of the home range survey conducted in Tomioka Town in 2014. Evacuation zones in the figure were classified on August 8, 2013. The mesh scale is 1 $km^2$.

Results for boar 50 were obtained during a survey conducted by the Ministry of the Environment in the 2013 fiscal year as reference data. Decontamination activities were not conducted in the 2013 fiscal year, and furthermore, there had been a lack of human activity for more than 2 years since the evacuation. The areas of the residential zone and home range were both 5 to 6 times those in Fukushima or Nihonmatsu City, and it is thus considered that the home range tends to expand in an environment where there is less pressure from humans.

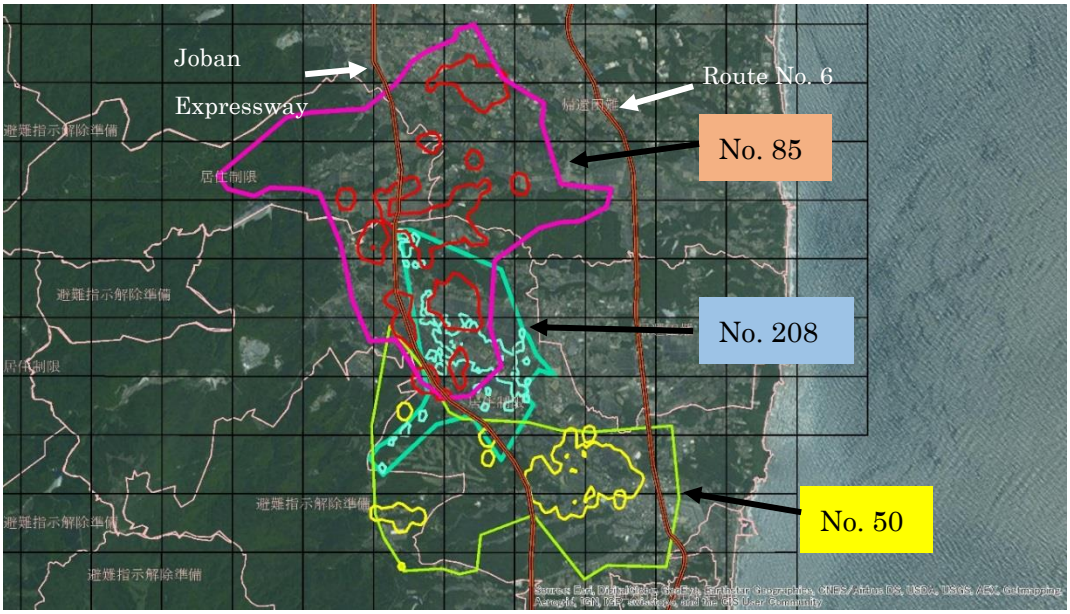


*Figure 14: Home range and land use in Tomioka Town*

Boar 85 was mounted with a collar in September 2014. Around that time, decontamination activities for restricted-residence areas began in Tomioka Town, and Figure 15 shows the effect of these activities on the home range. As described by the legend, the mean center of the home range is shown for three periods of one month each following

collaring. Perhaps owing to the effect of decontamination pressure, we find that the center of the home range moved from Tomioka Town to Okuma Town.

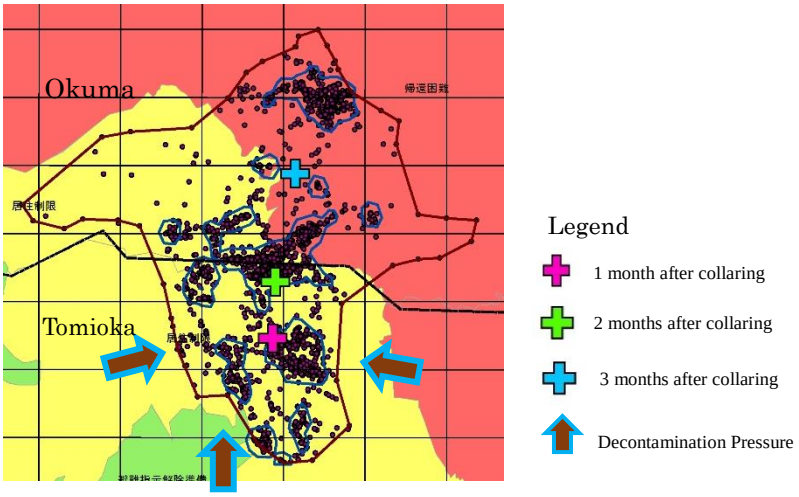


Movement distance of mean center from period 1 to period 3 was 2.3 km)

*Figure 15: Home range and mean center of movement of boar 85*

Figure 16 shows the home range of boar 208, to which a collar was attached on October 2014. The area of boar 208 was only one-third that of boar 85. During the collaring period, decontamination was underway in most of the home range, and perhaps because of the decontamination pressure acting from all four sides of the home range, the mean center of movement hardly moved at all during the third period.

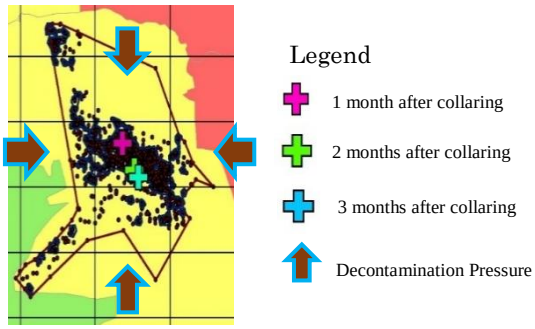


*Figure 16: Home range and mean center of movement of boar 208*

From the results of these surveys, it is considered that the size of the home range was affected by human activity or environmental factors. Figure 17 shows the areas of the residential zones and home ranges of boars captured both inside and outside the evacuation area. Boar 50 was under no pressure from people or decontamination. The home range of boar 85 expanded to Okuma Town owing to decontamination pressure. Boar 208 was under decontamination pressure from all four sides in the restricted-residence area. Boars 52 and 58 were in a peri-urban environment. Boars 66 and 67 were speculated to be affected by damage control pressure in a mountainous region. It seems that the size of the home range decreased with an increase in human pressure.

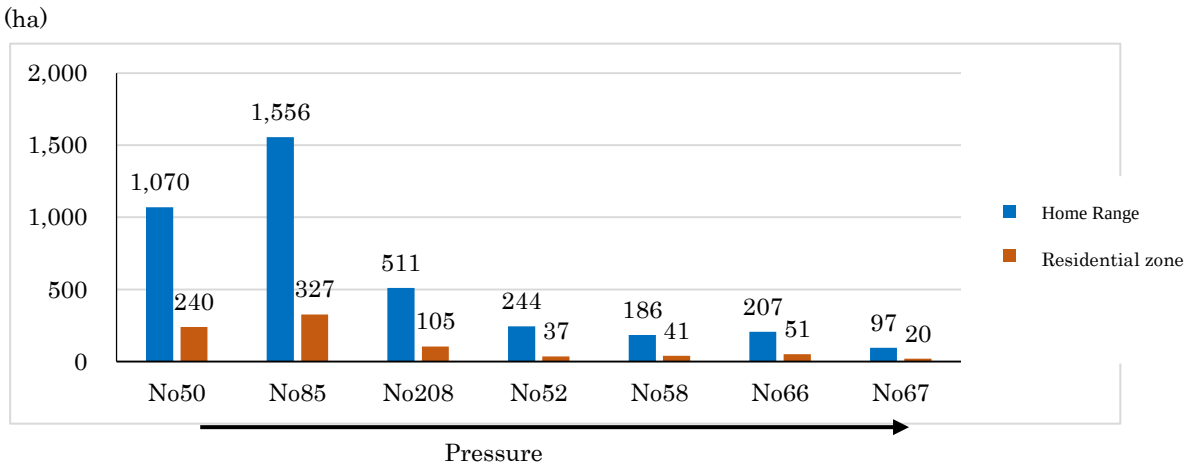


*Figure 17: Area comparison of the home range and residential zone*

*Table 1: Sample list*

| ID | No.50 | No.85 | No.208 | No.52 | No.58 | No.66 | No.67 |
|---|---|---|---|---|---|---|---|
| sex | ♂ | ♀ | ♀ | ♂ | ♂ | ♀ | ♀ |
| weight(kg) | 37 | 48 | 51 | 44 | 70 | 35 | 37 |
| GPS collar attached dates(day) | 81 | 99 | 117 | 99 | 50 | 110 | 34 |

The number of collared samples was small, and the sex, body weight, and duration that the collar was worn was different for each collared sample (Table 1). The size of the home range was affected by various factors, such as the sex and growth stage of the boar and the duration of GPS data. We therefore cannot provide concrete conclusions at this stage, but it is considered that the home range tended to shrink with increased human pressure.

# 3. FIP3: Project for studying decontamination technology for rivers and lakes

**Summary**

The third FIP organized knowledge on the behavior of and countermeasures for radionuclides (i.e., radiocaesium) in rivers and lakes. In rivers, where examples of countermeasure implementation were limited, a decontamination method was devised and tested and its effectiveness was confirmed. Additionally, the state of pollution was investigated in riverside parks and countermeasures were considered.

## 3.1. Purpose

The diffusion of radionuclides (especially radiocaesium) into the environment due to the Fukushima Daiichi Nuclear Power Plant accident has caused failures and anxiety in the use and management of rivers and lakes. For this reason, radionuclides in water, sediment, and aquatic products have been monitored and their behavior has been investigated mainly by the government and research institutions; countermeasures are currently being implemented. In the third FIP, radiocaesium countermeasures applicable to Fukushima Prefecture were organized using global knowledge, and a decontamination test was conducted because case examples of reducing external radiation exposure were limited for rivers in the prefecture. Additionally, the state of pollution was investigated in areas of public use (i.e., waterside parks) along other rivers, and the countermeasures were devised.

## 3.2. Details of Implementation

(1) Organization of knowledge on radiocaesium countermeasures in rivers and lakes

By referencing guidelines published by relevant ministries (MOE, 2014; MAFF, 2015) and the experience of the Chernobyl Nuclear Accident (IAEA, 2006), problems and possible countermeasures relating to the use of rivers and lakes in Fukushima Prefecture are organized in Table 1.

(2) Experimental test of radiocaesium decontamination in a river

a) Purpose

Among the problems raised in Table 1, the case examples of external exposure countermeasures in rivers are limited particularly for decontamination. A river is a major transport pathway for radiocaesium on land, and sediment containing radiocaesium is sometimes thickly deposited on floodplains. In general, only the top few centimeters of soil in

Fukushima Prefecture were decontaminated owing to radiocaesium accumulating only in that layer in farmland, forest, and residential areas. However, it is not clear whether this method is applicable to floodplains. We therefore tested the removal of topsoil on a floodplain as a decontamination method according to the depth distribution of radiocaesium.

*Table 1: Problems and possible countermeasures for the use of rivers and lakes*

| Problem | Related media | Possible countermeasures |
|---|---|---|
| Internal exposure via drinking water | Rivers and lakes | Change to alternative drinking water sources |
| Transfer of radiocaesium from irrigation water to crops and external exposure during farm work | Rivers and lakes | Mitigation of sediment inflow using silt fences, use of the sedimentation function of a dam |
| | Irrigation ponds | Silt fences, decontamination of bottom sediment |
| | Overall | Potassium fertilization of farmland |
| Internal exposure via the ingestion of aquatic products | Rivers and lakes | Restriction of the distribution and input of potassium (limited to closed lakes) |
| External exposure when using waterside areas (e.g., parks, roads, and housing) | Rivers | Access control, decontamination of floodplains, mitigation of deposition onto floodplains by promoting deposition onto riverbeds through riverbed excavation |
| | Lakes | Access control |
| | Irrigation ponds when being drained | Access control, decontamination of bottom sediment, covering with sand |
| Common to all problems | Sediment transportation prevention and decontamination of source areas of sediment. Risk communication for anxiety resulting from lack of information communication | |

b) Method

The test site was located at the most downstream position of the Kami-Oguni River, a third-order tributary of the Abukuma River, at a distance of 55 km northwest of the Fukushima Daiichi Nuclear Power Plant. The test section had a length of 170 m and an average width between banks of 15 m and a river channel width of 2 to 6 m under baseflow conditions (Figure 1). The left bank is used for an elementary school and its school road, and the right bank is used for an orchard. The floodplain is used for classes at the elementary school. The elementary school and the school road had been decontaminated before the present test.

The test was conducted according to the process outlined in Figure 2. Eighteen lateral lines were set at intervals of 10 m in the direction of the river flow (Figure 3), and the air dose rate 1 m above the ground on the lateral lines was measured using NaI scintillation survey meters without collimation. The measurement was conducted before decontamination, at the completion of decontamination, and 3 and 6 months after decontamination. Before decontamination and 6 months after decontamination, sediment was sampled from seven points on each of the floodplain and riverbed (Figure 3) and then subjected to radionuclide analysis using Ge semiconductor detectors. Sampled sediment was classified using sieves after the analysis, and the percentage weight of the mud fraction (i.e., silt and clay) relative to the total weight was then calculated. The water level was continuously monitored upstream of the test section.

The annual additional external exposure dose before and after decontamination was calculated as follows. The staying time was assumed to be 10 minutes per day for the school road on the left bank (35 hours per year) and 2 hours per week for the floodplain (100 hours per year). These values were multiplied by the average air dose rate after deducting the background value (0.04 μSv/h).

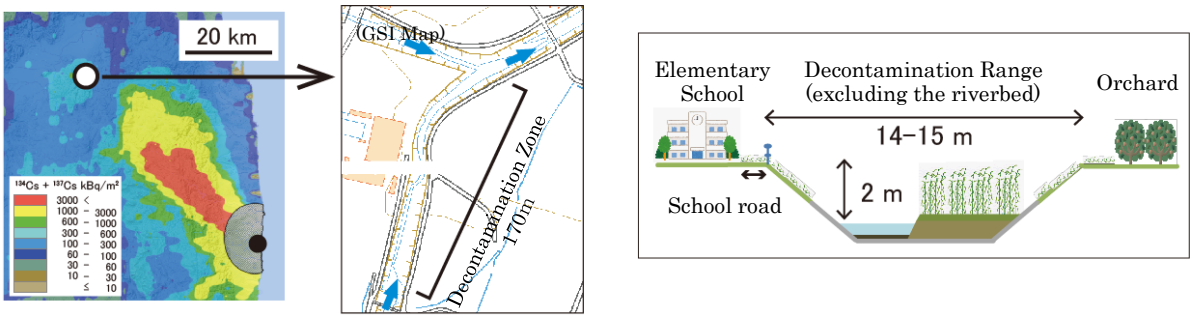


*Figure 1: Study site outline*

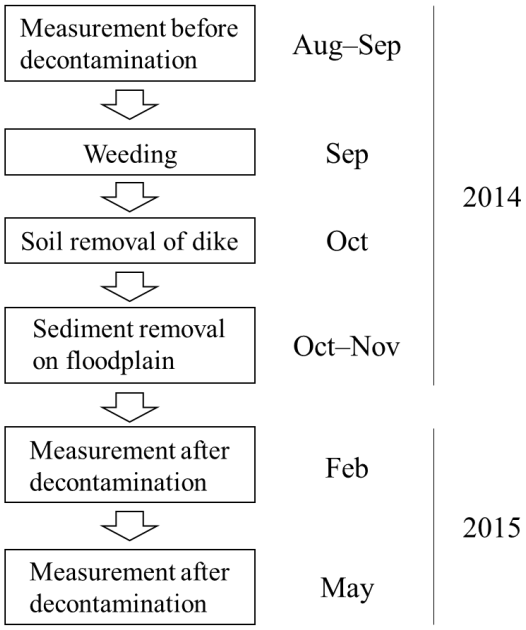


*Figure 2: Examination process*

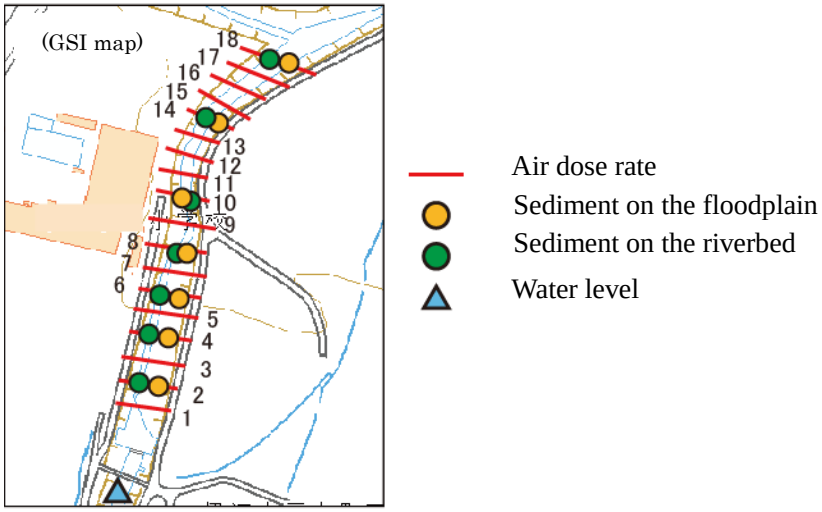


*Figure 3: Measurement points*

c) Results and discussion

The vertical distribution of the activity concentration of radiocaesium on the floodplain is shown in Figure 4. Along lines 4, 6, and 8, the concentration exceeded 10,000 Bq/kg (caesium-137) to a depth of 15 cm. In the layers corresponding to that depth, the percentage mud fraction was high at 31% to 55% (Figure 4). Because radiocaesium has the nature of being strongly adsorbed to clay and silt (He and Walling, 1996), it is unlikely that

radiocaesium penetrated below a depth of 10 cm at points with a high percentage of the mud fraction. Along lines 10 and 14, the concentration peaks were distributed below a depth of 10 cm with a low percentage of the mud fraction of 2% to 17%. However, it is unlikely that caesium-137 penetrated below a depth of 10 cm sufficiently to form the layers with a concentration exceeding 5000 Bq/kg. Therefore, those surface sediments were probably deposited during floods after the initial deposition of radiocaesium. In consideration of the vertical distribution, we set a removal depth of 15 to 35 cm on the floodplain. A similar vertical distribution of radiocaesium has been reported on floodplains (Tanaka et al., 2015; Konoplev et al., 2016), indicating that the investigation of the vertical distribution in advance of decontamination is important.

The vertical distribution of radiocaesium activity concentration on the riverbed is shown in Figure 5. In contrast to the distribution for the floodplain, the distribution for the riverbed was nearly uniform. Relatively low values of the radiocaesium activity concentration and percentage of the mud fraction were observed, with 70% of samples having a concentration lower than 1000 Bq/kg and a mud fraction lower than 5%. Mikami et al. (2014) also reported a difference in distributions between a floodplain and riverbed for a river 4 km to the east of the test site, and indicated two factors responsible for the difference. One factor is that mud with a high radiocaesium concentration tends to be easily discharged on a riverbed under running water. The other is the promotion of sedimentation on floodplains by the plant community, which acts as an obstacle to the flow of water and suspended solids during floods. In consideration that river water provides a shield against gamma rays emitted from the riverbed, we did not decontaminate the riverbed in this test.

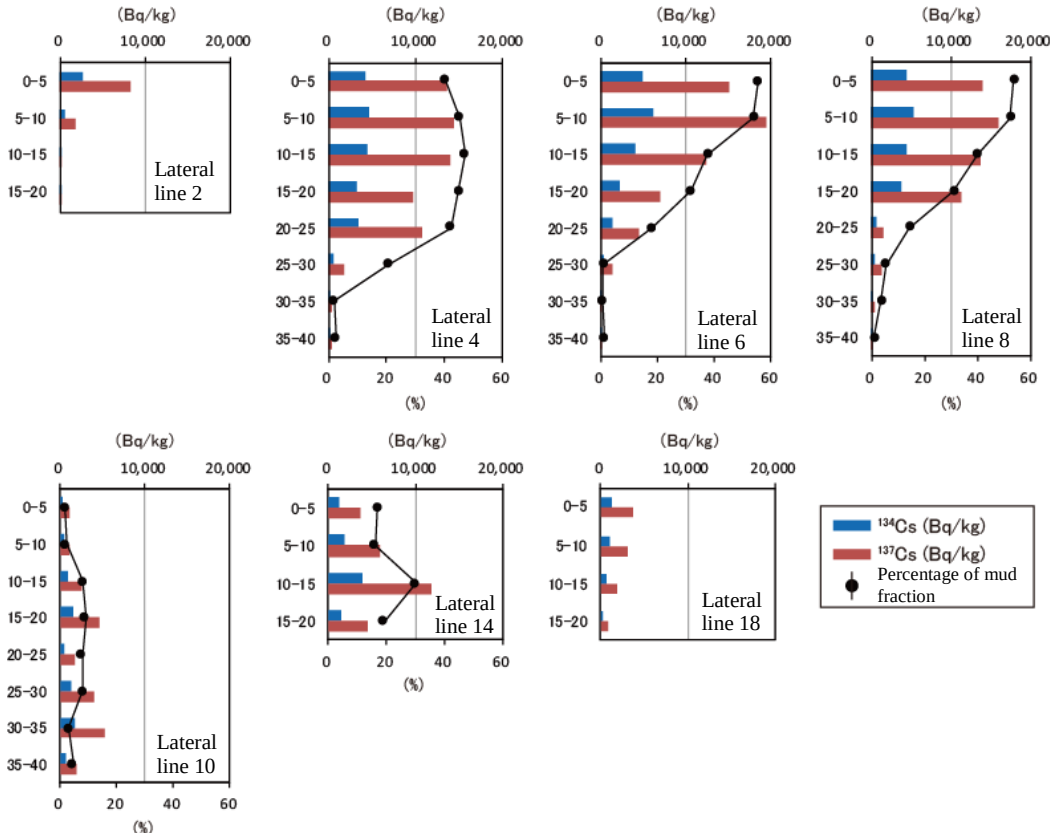


*Figure 4: Vertical distribution of the activity concentration of radiocaesium in floodplain sediment before decontamination*

The distribution of the air dose rates 1 m above the ground is shown in Figure 6. The average value and standard deviation were 0.66 ± 0.22 μSv/h before decontamination but decreased by half to 0.34 ± 0.11 μSv/h after decontamination, confirming the effectiveness of the test method. There was hardly any change in the value of 0.34 ± 0.12 μSv/h three months after decontamination. Afterward, although there was a flood in March 2015, the activity concentration of caesium-137 remained low in sediment at a depth of 0 to 20 cm on the floodplain (860 ± 760 Bq/kg) and in sediment at a depth of 0 to 5 cm on the riverbed (660 ± 720 Bq/kg). As a result, the air dose rate six months after decontamination (0.30 ± 0.12 μSv/h) was hardly different from that at the completion of decontamination. The effects of decontamination have therefore been maintained.

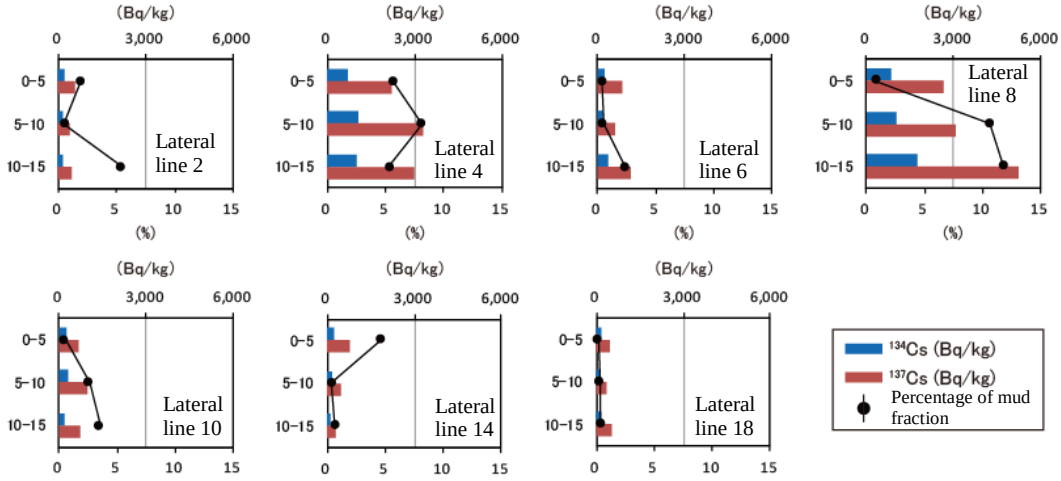


*Figure 5: Vertical distribution of the activity concentration of radiocaesium in riverbed sediment before decontamination*

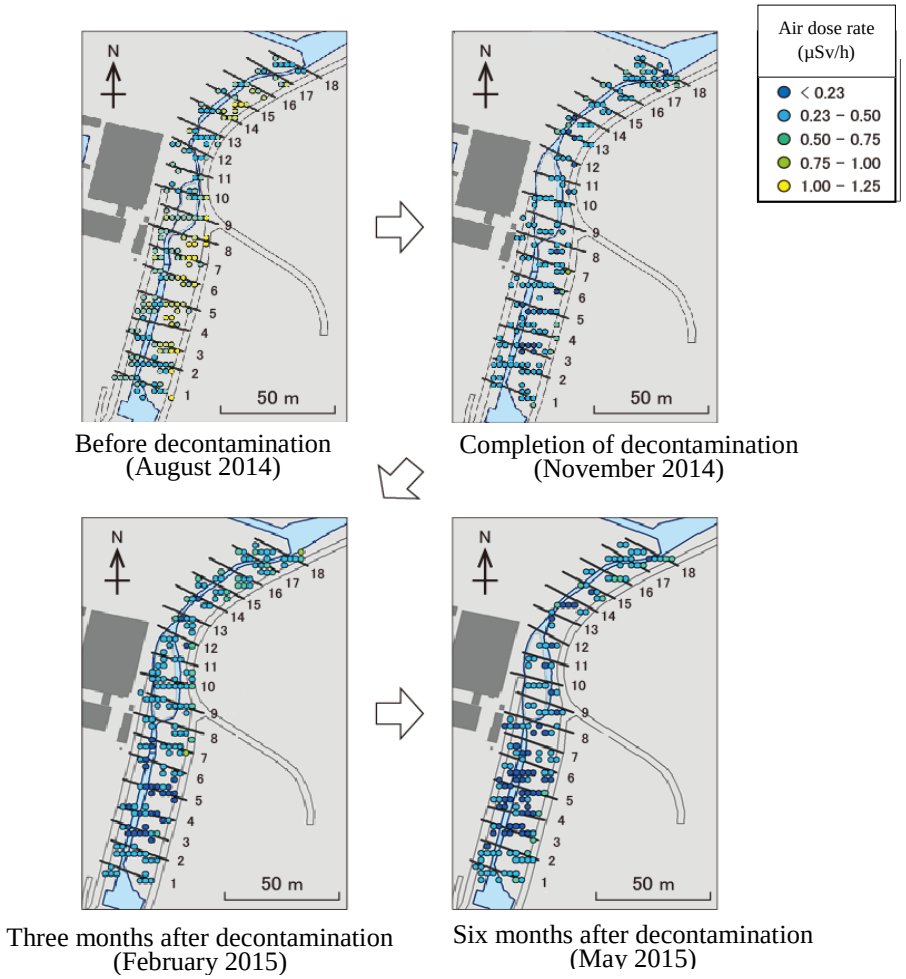


*Figure 6: Temporal change in the air dose rate*

Annual additional external exposure doses for using the school road and floodplain were estimated to be 0.089 mSv/year before decontamination and 0.034 mSv/year after decontamination, resulting in 62% reduction of the exposure dose. In the town where the test was conducted, an average exposure dose of 1.23 mSv/year was obtained for the period from July 2013 to June 2014 using a glass dosimeter (Date City, 2015). The use of the test site corresponded to 7.2% of the exposure dose in daily life before decontamination and 2.7% after decontamination. Therefore, reduction of the exposure dose by decontamination was estimated to be 4.5% of the exposure dose in daily life.

(3) State of pollution in river parks and examination of countermeasure methods

a) Purpose

As stated in section (2), radiocaesium sometimes accumulates along with sediment deposition on riversides. Because upstream areas are appreciably polluted in the coastal region of eastern Fukushima Prefecture, there is concern about the possibility that the floodplains in the downstream area are more contaminated than the surrounding area. Riverside parks are one type of floodplain area used by people. We therefore investigated the state of pollution and the effect of floods on riverside parks in the coastal region, and discussed countermeasures.

b) Method

Study sites were located at two points downstream of the Niida River, one of the major rivers in the coastal region (Figure 7). Park A is located along the main stream of the Niida River, while Park B is located along the Mizunashi River, a first-order tributary of the Niida River. A dam is located 5 km upstream from park B. Parks A and B have areas of 2.7 and 1.6 ha, respectively. In August 2015 before a flood and in September 2015 after the flood, the air dose rate was measured 5 cm and 1 m above the ground using a portable gamma-ray measuring device (Gamma Plotter H, Japan Radiation Engineering Co., Ltd.). At the same time, the additional external exposure dose was measured using a dosimeter (Dose e nano, Fuji Electric) for various activities, including recreation, walks, and park maintenance.

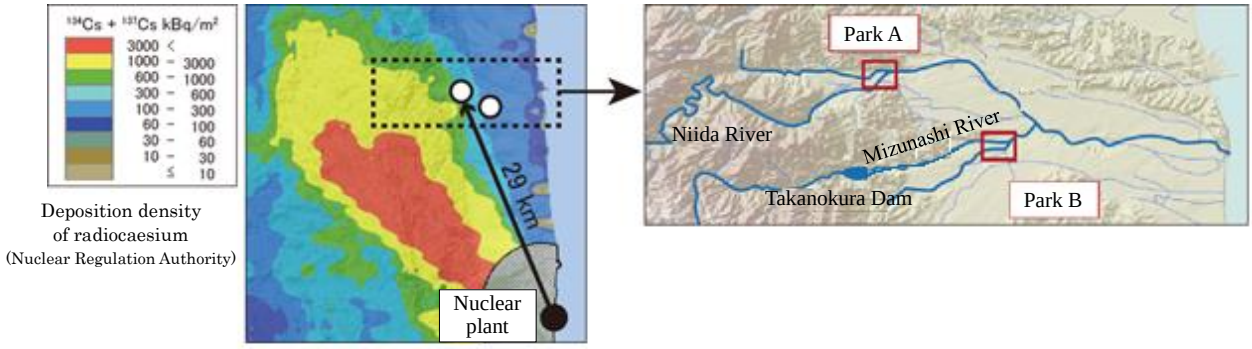


*Figure 7: Location map of study sites*

c) Results and Discussion

The distribution of the air dose rate in park A during August and September 2015 is shown in Figure 8. In August 2015, the air dose rate was 0.20–2.14 μSv/h at a height of 5 cm and 0.22–1.75 μSv/h at a height of 1 m. Relatively high values exceeding 1.0 μSv/h were distributed primarily in the northeastern part of the park along the river, suggesting the accumulation of radiocaesium by sediment deposition. However, after a flood in September 2015, the values fell below 1.0 μSv/h at many points on the riverside and in the northeastern part of the park. This is likely attributed to the deposition of a large quantity of coarse particles (mainly sand) along the river and erosion up to several tens of centimeters in the northeastern part of the park. The appreciable deposition and erosion were caused by the extreme flood (resulting from 385 mm precipitation over 6 days recorded at a weather station 7 km to the southeast).

For the additional external exposure dose, the value of use situations before the flood was 0.092 mSv/year under the assumption of a staying time of 180 hours per year, while after the flood, it fell 30% to 0.064 mSv/year. In this city where park A was located, an average exposure dose of 0.44 mSv/year has been measured using a glass dosimeter in the period from July to September 2015 (Minami-Soma City, 2016). The use of park A corresponded to 21% of the exposure dose in daily life before the flood and 15% after the flood. In considering countermeasures for park A, it is noted that although the high air dose rate was still distributed along the river after the flood, the utilization of the area along the river seems to be limited by the lush reed community along the river. Moreover, as described above, the exposure dose was estimated to be less than 0.1 mSv/year. We therefore conclude that there is little to fear under present conditions. Meanwhile, there is the possibility of recontamination by radioactivity sediment on the floodplain in the future. Monitoring and future prediction are effective responses to such concerns.

The distribution of the air dose rate in park B during August and September 2015 is

shown in Figure 9. In August 2015, the air dose rate was 0.18–1.06 μSv/h at a height of 5 cm and 0.23–0.69 μSv/h at a height of 1 m, except for the residential area to the south of the park. In contrast to the distribution in park A, the distribution in park B was nearly uniform, and the air dose rate along the river was not high. In the extreme flood of September 2015, the northern half of park B appeared to be inundated according to the distribution of plant residue washed down, but sediment and erosion were rarely found. As a result, there was almost no change in the air dose rate even after the flood. Similarly, for the additional external exposure dose, the value of use situations hardly changed from 0.047 mSv/year before the flood to 0.046 mSv/year after the flood (assuming a staying time of 190 hours per year). It is inferred that one factor responsible for the small change was the capture of suspended solids by the dam upstream of park B. Considering the low exposure dose and weak effect of floods, we conclude that there is little to fear under the present conditions also in park B.


August 2015 (height of 5 cm) August 2015 (height of 1 m)

September 2015 (height of 5 cm) September 2015 (height of 1 m)

*Figure 8: Distribution of the air dose rate in park A. The white broken line represents the park area.*

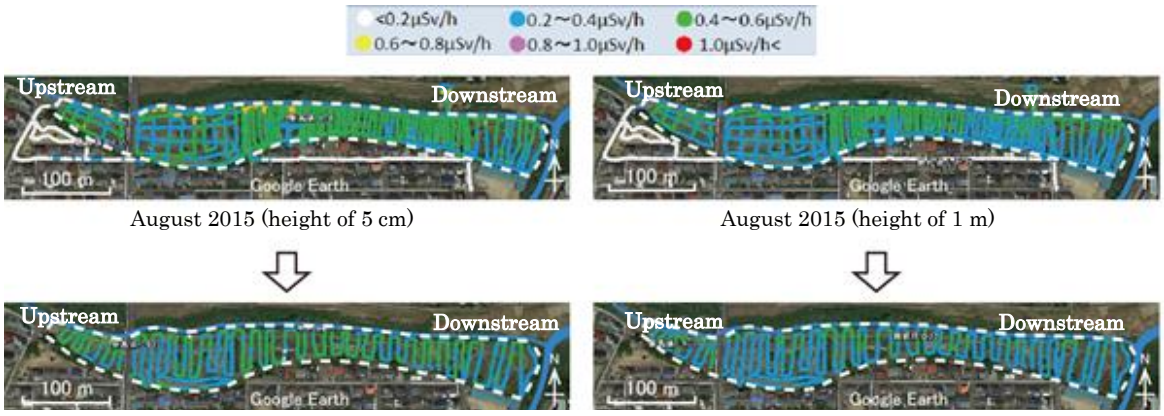


August 2015 (height of 5 cm) August 2015 (height of 1 m)

September 2015 (height of 5 cm) September 2015 (height of 1 m)

*Figure 9: Distribution of the air dose rate in park B. The white broken line represents the park area.*

References

Date City (2015) Date Recovery/Rejuvenation News (No. 22).

http://www.city.date.fukushima.jp/soshiki/12/763.html. (in Japanese)

He Q., Walling D. E. (1996) Interpreting particle size effects in the adsorption of $^{137}Cs$ and unsupported $^{210}Pb$ by mineral soils and sediments. Journal of Environmental Radioactivity, 30, 117-137.

IAEA (2006) Environmental consequences of the Chernobyl accident and their remediation: Twenty years of experience report of the Chernobyl forum expert group 'environment'. Vienna.

MOE (2014) Guidelines for Decontamination. https://josen.env.go.jp/material/. (in Japanese)

Konoplev, A., Golosov, V., Laptev, G., Nanba, K., Onda, Y., Takase, T., Wakiyama Y., Yoshimura, K. (2016) Behavior of accidentally released radiocaesium in soil–water environment: Looking at Fukushima from a Chernobyl perspective. Journal of environmental radioactivity, 151, 568-578.

Mikami, T., Maie, N., Shimada, H., Kakizaki, T., Takamatsu, R., Itou, N., Tanaka, K., Shima, E. (2014) Influence of microtopography on radioactive caesium accumulation in waterside lands: Case study of second order tributaries of the Abukuma River flowing through Fukushima Prefecture. Society on Water Environment Journal, 37 (6), 259-264. (in Japanese)

Minamisoma City (2016) 2015 No. 2 individual cumulative dose measurement (7/2015 – 9/2015) results. Cityhttp://www.city.minamisoma.lg.jp/index.cfm/10,28438,61,367,html. (in Japanese)

MAFF (2015) Technical Manual on Countermeasures for Radioactive Material in Ponds. http://www.maff.go.jp/j/nousin/saigai/tamemanu_zentai.html. (in Japanese)

Tanaka, K., Kondo, H., Sakaguchi, A., Takahashi, Y. (2015) Cumulative history recorded in the depth distribution of radiocaesium in sediments deposited on a sandbar. Journal of Environmental Radioactivity, 150, 213-219.

# 4. FIP4: Development of environmental mapping technology with GPS walking surveys

**Summary**

Fukushima Prefecture developed environmental mapping technology with GPS walking surveys as a tool for surveying the regional distribution of air dose rates.

This report covers the results of parameter verification necessary for the development of this technology and the history of development.

## 4.1. Purpose

To grasp the air dose rate (hereinafter simply referred to as the dose rate) in Fukushima Prefecture after the accident at the Fukushima Daiichi Nuclear Power Plant, we have conducted fixed-point measurements with monitoring posts and dose rate measurements in car-borne surveys using the GPS-linked dose rate measurement device KURAMA (Kyoto University RAdiation MApping System), and have provided information to prefecture residents on the prefecture homepage (Image 1, Figure 1).


*Image 1: Example of monitoring currently being conducted*

*(a): Example of a fixed-point measurement*

*(using a real-time dose-rate measurement system)*

*(b): Example of a car-borne survey*

*(KURAMA-II installed on the back of a local bus)*

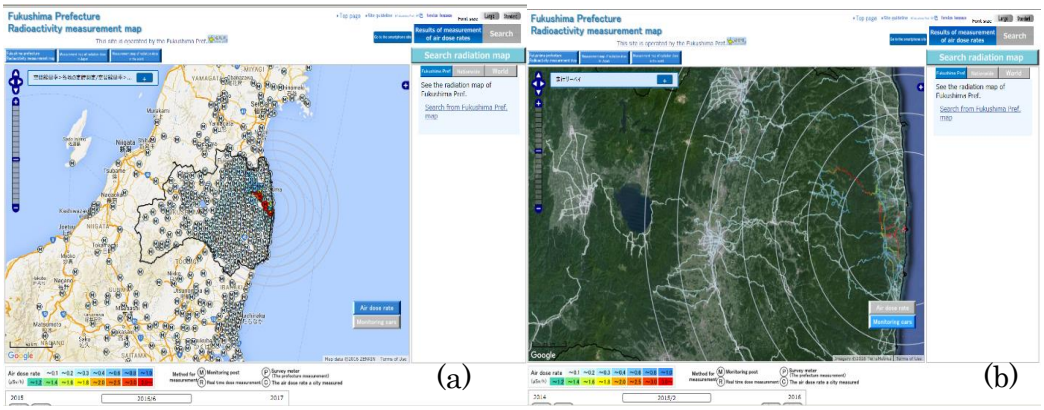


*Figure 1: Radioactivity measurement in Fukushima Prefecture*
*(http://fukushima-radioactivity.jp/pc/)*
*(a): Example of a fixed-point measurement*
*(b): Example of a traveling survey*

As of March 2016, measurements are being made at 3500 fixed points with monitoring posts in Fukushima Prefecture. Car-borne surveys using local buses are also being conducted with the purpose of interpolating the fixed-point measurements.

It is, however, difficult to conduct fixed-point measurements or car-borne surveys in some places, including parks, forests, and alleys near residential areas, and dose rates sometimes differ between fixed measuring points at the same facility or site (Figure 2). For these reasons, in addition to fixed-point measurements and car-borne surveys, we require measurement technology with which to grasp a more detailed distribution of dose rates, and we need to present the measurement results in a format that is easy to understand.

Therefore, to employ interpolation to obtain dose rates for parks, forests, and alleys near residential areas where fixed-point measurements and car-borne surveys are difficult, we developed environmental mapping technology using GPS walking surveys together with unmanned aerial vehicles (UAVs) developed by the IAEA.

The prefecture and IAEA have shared the development of environmental mapping technology with GPS walking surveys (FIP4) and environmental mapping technology with unmanned aerial vehicles (FCP3), and by combining these technologies and visualizing measurement results, we were able to create dose distribution maps that are more detailed and effective.

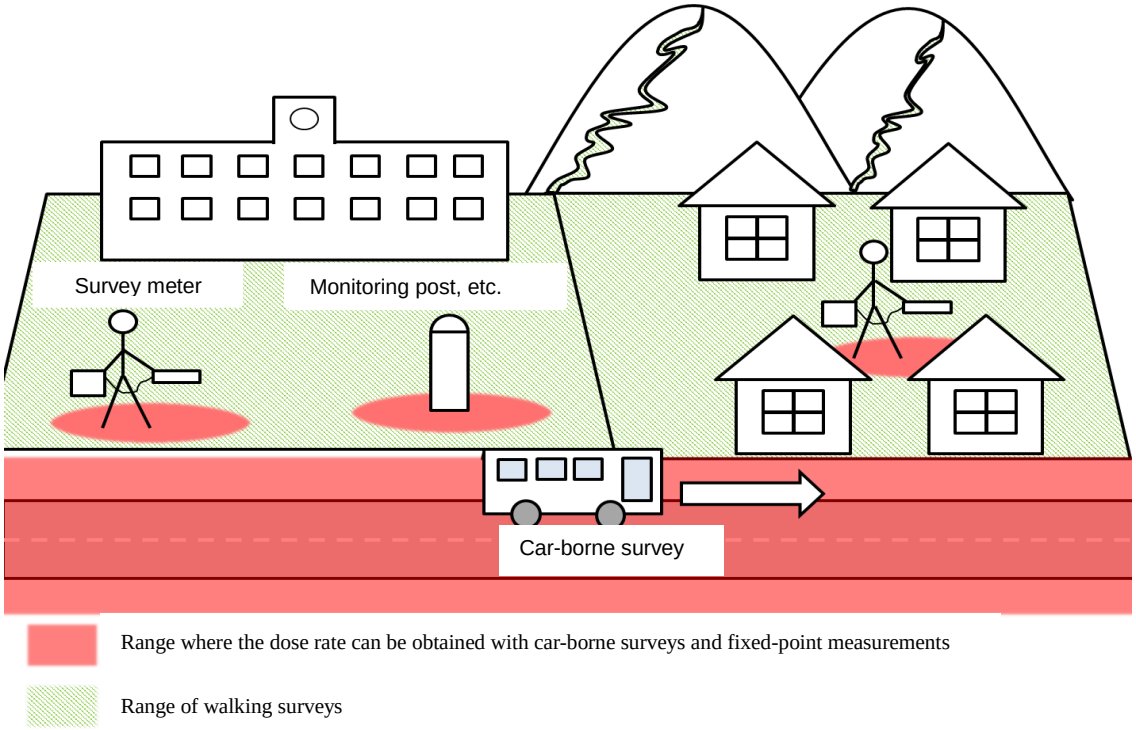


*Figure 2: Measurement ranges of conventional measurement methods*

## 4.2. Implementation Details

(1) Development of equipment

We used the KURAMA-II, which was developed by Kyoto University, for walking surveys, and assembled five pieces of equipment in a way suited to walking surveys (Image 2). The orange backpack contains a CsI (T1) scintillation detector, which is a low-dose-rate detector, and a high-precision GPS unit.

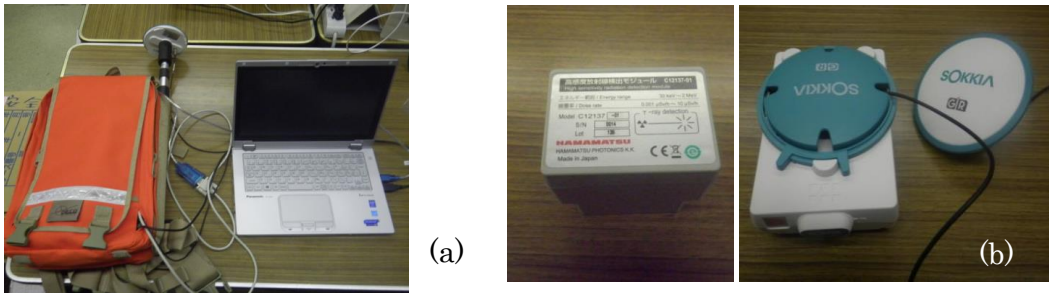


*Image 2: Walking survey equipment*

*(a): Appearance of the devices*

*(b): Low-dose-rate CsI detector (Hamamatsu Photonics K.K. C12137-01) and high-precision GPS unit (SOKKIA GIR1600)*

The measurement screen is shown in Figure 3. The measurement interval may be selected as 3 seconds, 5 seconds, and so on. At the start of the measurement, information such as the current position and dose rate are recorded to a notebook computer, and the position information, dose rate, trends, and mapping results are displayed on the computer screen.

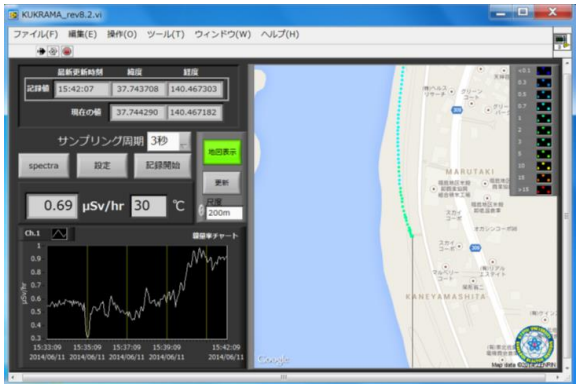


*Figure 3: Display screen on a personal computer*

Measurers can look at the screen to check the measurement position and dose rate while conducting detailed measurements.

(2) Development of mapping technology using geographic information systems (GISs)

We conducted a specification study and developed a GIS tool for capturing, combining, and mapping the dose rate and position information gained from walking surveys and UAVs. An overview of the tool is shown in Figure 4.

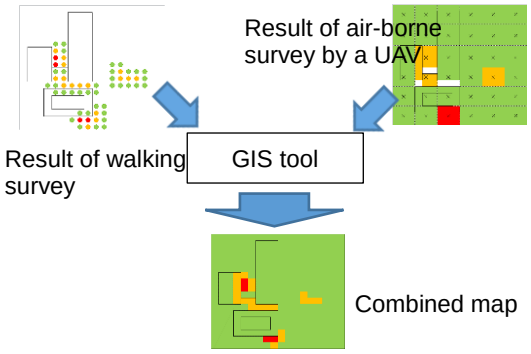


*Figure 4: Overview of the GIS tool*

| | 年月日 | 時間 | 緯度 | 経度 | 標高 | 速度 | 方位 | 線量率 | 補正線量率 | 検出器温度 |
|---|---|---|---|---|---|---|---|---|---|---|
| 2 | 2013/12/12 | 13:58:19 | 37.478633 | 140.857184 | 27.2 | 0.7 | 202.37 | 1.9 | | 10.37 |
| 3 | 2013/12/12 | 13:58:22 | 37.478629 | 140.85718 | 27.1 | 0.4 | 213.87 | 1.85 | | 10.37 |
| 4 | 2013/12/12 | 13:58:25 | 37.478631 | 140.857181 | 26.9 | 0.5 | 341.95 | 1.82 | | 10.37 |
| 5 | 2013/12/12 | 13:58:28 | 37.478629 | 140.857186 | 27.2 | 4.4 | 148.05 | 1.93 | | 10.37 |
| 6 | 2013/12/12 | 13:58:31 | 37.478625 | 140.857184 | 27.3 | 6 | 192.24 | 2.09 | | 10.37 |
| 7 | 2013/12/12 | 13:58:34 | 37.478624 | 140.85721 | 28.1 | 3.2 | 58.5 | 2.1 | | 10.37 |
| 8 | 2013/12/12 | 13:58:37 | 37.478625 | 140.857241 | 28.2 | 8.9 | 111.9 | 2.48 | | 10.37 |
| 9 | 2013/12/12 | 13:58:40 | 37.478628 | 140.857269 | 28.3 | 8.2 | 125.81 | 2.55 | | 10.38 |
| 10 | 2013/12/12 | 13:58:43 | 37.478705 | 140.857263 | 28.2 | 8.4 | 168.38 | 2.67 | | 10.38 |
| 11 | 2013/12/12 | 13:58:46 | 37.478758 | 140.857284 | 28.3 | 8.7 | 155.82 | 2.75 | | 10.38 |
| 12 | 2013/12/12 | 13:58:49 | 37.478735 | 140.857319 | 28.2 | 8.4 | 112.31 | 2.9 | | 10.39 |
| 13 | 2013/12/12 | 13:58:52 | 37.478717 | 140.857348 | 28.2 | 7.5 | 132.18 | 2.7 | | 10.39 |
| 14 | 2013/12/12 | 13:58:55 | 37.4787 | 140.857374 | 28.1 | 8.4 | 133.22 | 2.68 | | 10.39 |
| 15 | 2013/12/12 | 13:58:58 | 37.478684 | 140.857384 | 28.2 | 7 | 130.09 | 2.22 | | 10.39 |
| 16 | 2013/12/12 | 13:59:01 | 37.478682 | 140.857384 | 28.2 | 0.8 | 222.58 | 2.13 | | 10.39 |

*Figure 5: Data including the dose rate*

It is possible to produce a contour map using the GIS tool. Data in comma-separated-value format recorded in walking surveys are converted to Microsoft Excel file format (Figure 5), and point data with dose rate information are created from the latitudinal and longitudinal information contained in the data (Figure 6). With the GIS tool, it is possible to estimate the dose rate at unmeasured positions and to produce contour maps from the point data created using any interpolation algorithm, such as a Kriging or IDW algorithm (Figure 7).

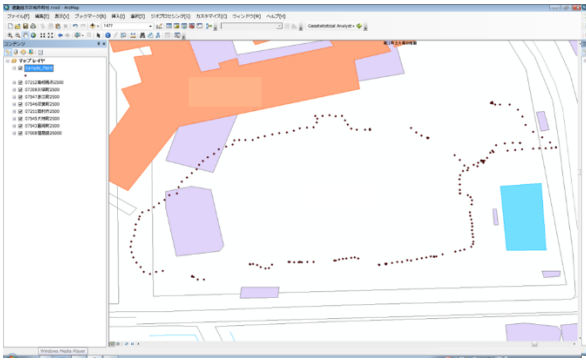

*Figure 6: Map data and dose plot*

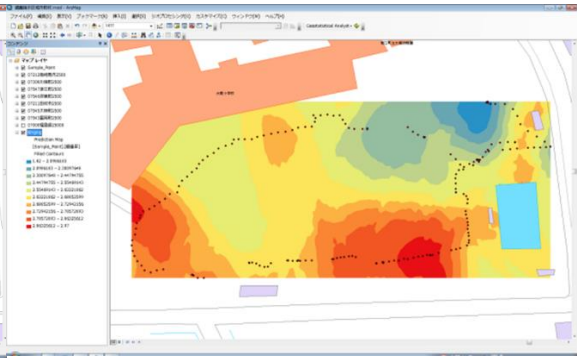

*Figure 7: Interpolated dose map*

The tool was made with the purpose of combining and mapping walking survey data and UAV data. However, because a method of evaluating aerial surveys with UAVs has yet to be determined, we will reexamine this purpose after the development of the UAV is complete.

(3) Gathering parameters necessary for walking surveys

We conducted a field test of walking surveys, and gathered data for evaluation and analysis (Picture 3). Data were gathered to check the direction characteristics and appropriate measurement density, as well as to determine correction factors.

*Picture 3: View of a walking survey*

a) Checking direction characteristics

Shielding from the measurers themselves affects the contribution from the radiation source depending on the walking direction in walking surveys (Figure 8). Walking surveys were therefore conducted by changing the walking speed and by walking back and forth so as to straddle the radiation source and check the effect of direction characteristics.

As a result, while shifts occurred in places where peaks appeared, they fell within a range of about 2 meters, and measurements showed that the maximum value of the dose rate was nearly the same during forward and reverse passes (Figure 9). We also confirmed that reducing the walking speed caused the peaks of the dose rate distribution to grow sharply (Figures 10 and 11).

According to the above results, we consider the effect of direction characteristics on walking survey measurements made at a constant walking speed to be weak.

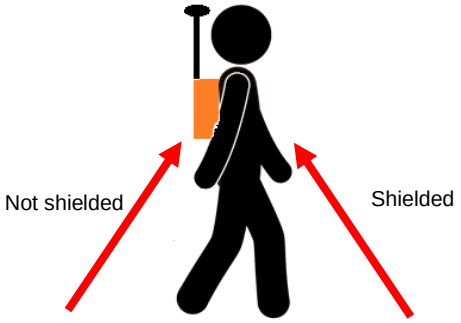


*Figure 8: Measurement of direction characteristics*

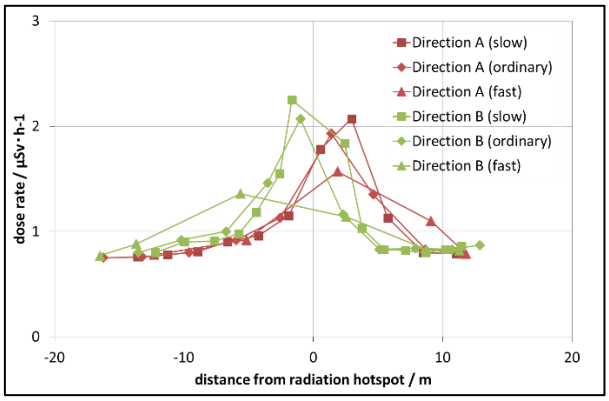


*Figure 9: Measurements after changing speed and direction*

*Figure 10: Change in walking speed*

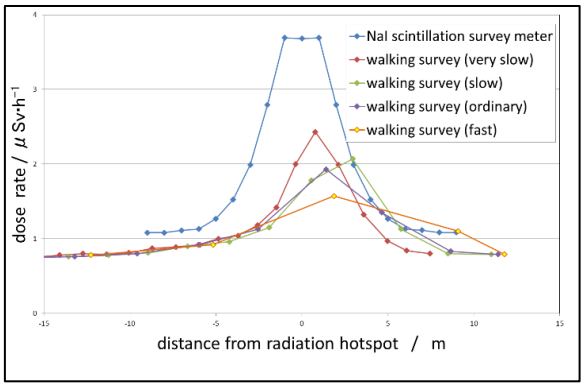


*Figure 11: Change in measurements due to walking speed*

b) Determination of correction factors in a comparison test with survey meters

We assumed measurements made with a NaI(Tl) scintillation survey meter (TCS-172B) at a height of 1 m to be the most reliable, and the survey meter was calibrated with traceability. We compared measurements made using a survey meter with those obtained in a walking survey (Image 4). A comparison was made at several points with differing dose rates. At each point, we faced north, south, east, and west and made measurements five times in each direction to mitigate direction characteristics. We then took the average value for all directions as the measurement for that point. We next plotted the measurements of walking surveys against the survey meter to determine the correction factor.

(a)

(b)

*Image 4: Images of measuring*

*(a): Measurement with a survey meter*

*(b): Measurement in a walking survey*

*Both measurements were made facing four directions*

The results of the comparison are shown in Figure 12. There was good linearity between the measurements of walking surveys and the survey meter below a survey meter measurement of 1 μSv/h, whereas the linearity deteriorated above approximately 1 μSv/h. This phenomenon is due to count loss caused by excessive radiation incidence on the CsI detector.

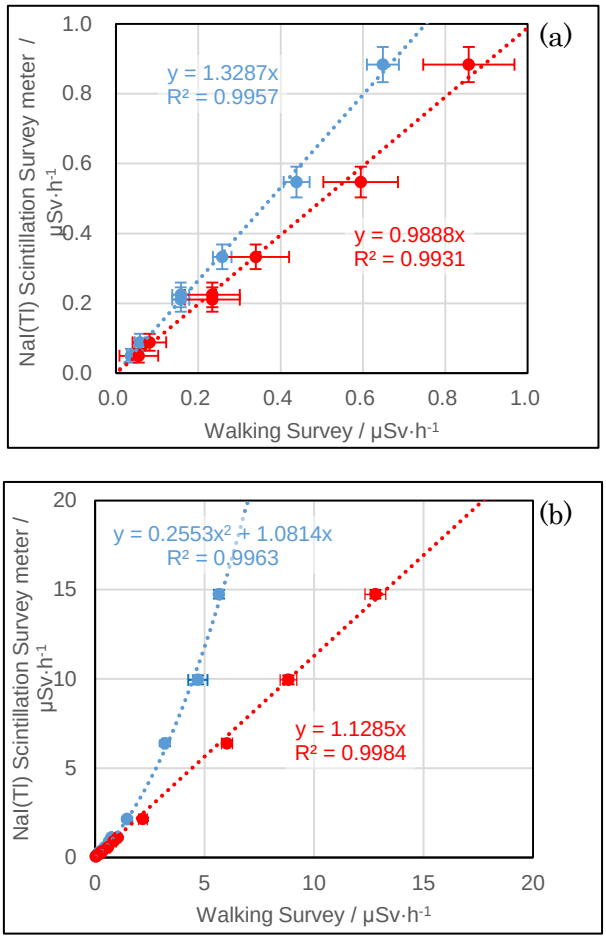


*Figure 12: Comparison of measurements of the survey meter and walking survey*

*(a): Chart plotting data below 1 μSv/h*

*(b): Chart plotting all data*

- *Comparison of the measurements of the low-dose-rate CsI detector and NaI survey meter*
- *Comparison of the measurements of the high-dose-rate CsI detector and NaI survey meter*

*Note that the approximate curve is not affected by the self-dose from the measurement detector, with the intercept being zero.*


*Image 5: High-dose-rate CsI detector*
*(Hamamatsu Photonics K.K. C12137)*

In light of the above results, we changed the detector to a high-dose-rate CsI detector (Image 5) and compared the results obtained using the survey meter with measurement results of walking surveys again. The results are shown in Figure 12(b). We confirmed that as a result of changing the detector, the linearity of walking survey measurements against survey meter measurements is obtained even in the high dose range. We also confirmed that the high-dose CsI detector can make better measurements than the low-dose rate CsI detector in the high dose range in field tests. This is also confirmed in Figure 13, which shows the walking survey results having changed detectors at the same geographic point. The maximum indicated value is higher for the high-dose-rate CsI detector than for the low-dose-rate CsI detector, and the high-dose-rate area represented by red markers appears, indicating that measurements are made without counting loss of radiation.

According to the above comparisons, we set the correction factor of walking surveys to 1.3 when using the low-dose-rate CsI detector at points with a dose rate less than 1 μSv/h and 1.1 when using the high-dose-rate CsI detector.

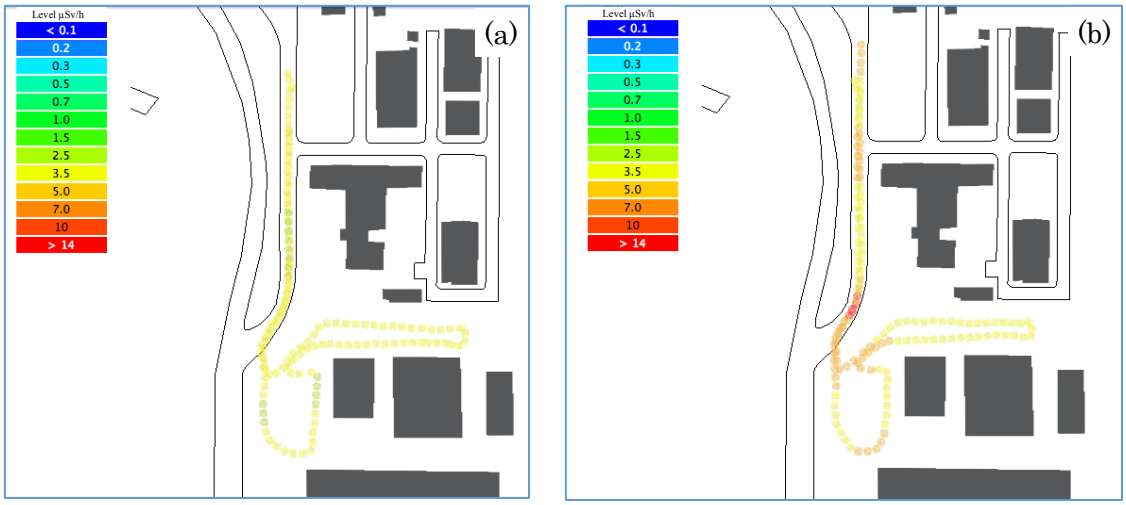


*Figure 13: Walking surveys having changed the detector*

*(a): Walking survey with the low-dose-rate CsI detector*

*The indicated value range is 2.77 to 5.99 μSv/h.*

*(b): Walking survey with the high-dose-rate CsI detector*

*The indicated value range is 5.00 to 29.5 μSv/h.*

c) Confirming variations in measurements

We conducted-fixed point measurements to confirm variations in measurements for a measurement time of 3 seconds in the low dose rate range. Fixed-point measurements were made with both the low-dose-rate CsI detector and the high-dose-rate CsI detector.

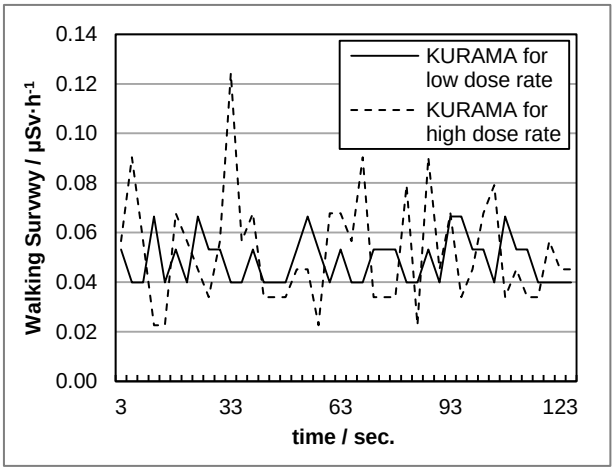


*Figure 14: Confirming variations in measurements*

Results showed that the variation in measurement results was larger for the high-dose-rate CsI detector at points with a low dose rate (Figure 14). The variation coefficient obtained from dividing the standard deviation of measurements by the average value was 19.7% for the low-dose-rate CsI detector but 42.7% for the high-dose-rate detector. Error in measurements made with the low-dose-rate detector was small because of the high counting rate achieved with the large crystal while error in measurements made with the high-dose-rate detector was large because of the small

counting rate achieved with the small crystal.

On this basis, we decided to use the low-dose-rate CsI detector, which has a small variation at low dose rates, at geographic points with a dose rate less than 1 μSv/h, and to use the high-dose-rate CsI detector at geographic points with a dose rate greater than 1 μSv/h.

(4) Conducting walking surveys

With the purpose of studying the operation of walking surveys and acquiring basic data, we conducted walking surveys at places with differing conditions. Examples of such walking surveys are described below.

a) Walking survey in western Fukushima City

We conducted a walking survey on a trial basis in western Fukushima City. At the center of this geographic area is a surface paved with asphalt, with ditches along the edges. There were no obstructions on the outside of the asphalt surface, leaving the surface wide open and surrounded by grass. Results of a walking survey conducted at this geographic point are shown in Figure 15. The paved surface at the center of the range of the walking survey had a low dose rate compared with that of the surroundings. It is considered that this low dose rate is due to the easy decontamination of the paved surface and the strong effect of weathering. In addition, the radiation dose in the vicinity of the ditch was higher than that of the surroundings. This is probably because there was an inflow of radioactive material from the surrounding area. We conducted a high-density walking survey and tested interpolation with a GIS tool (Figure 16). Interpolation was conducted with IDW. The interpolated radiation dose rate in the paved area was low, and the dose rate in the vicinity of the ditch was high.

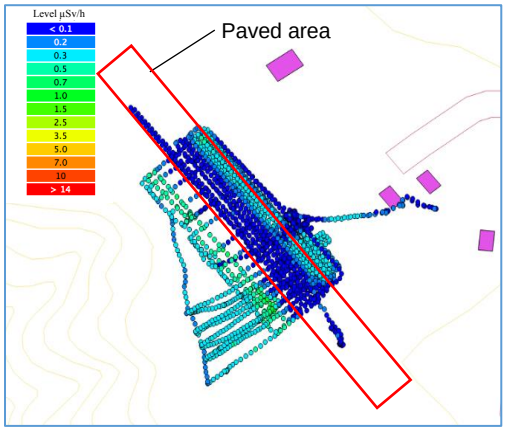


*Figure 15: Results of a walking survey in western Fukushima City*

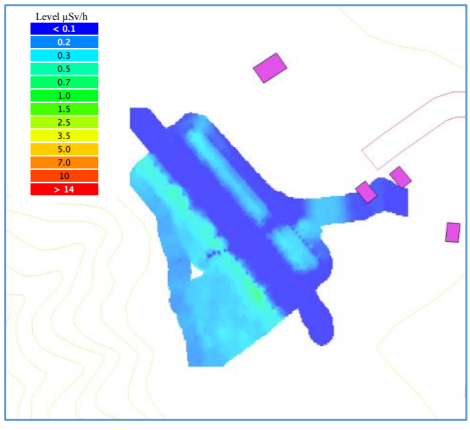


*Figure 16: Results of interpolation with IDW*

b) Walking survey in the periphery of a temporary storage area

We conducted a walking survey in a temporary storage area and its periphery in the Nakadori region of Fukushima Prefecture (Figure 17). The area inside the red frame in the figure is the temporary storage area. The dose rate near the temporary storage area was equal to or less than the dose rate in the periphery, and no effect of decontamination on the outside area was seen in this temporary storage area.

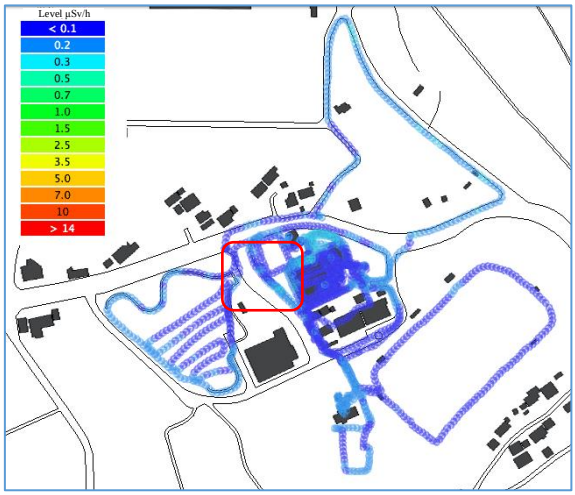


*Figure 17: Dose map (with the temporary storage area indicated by the red frame)*

c) Walking survey in the Hamadori region (outside the evacuation zone)

We conducted a walking survey around rivers in the Hamadori region of Fukushima Prefecture (outside the evacuation zone) (Figures 18 and 19). There is a paved surface on the left side of the figure, with the rest of the study area being gravel or grassland. The dose rate was low on the paved surface and nearly uniform in other areas.

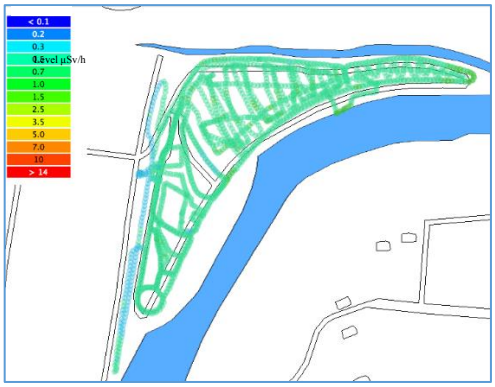


*Figure 18: Dose map*

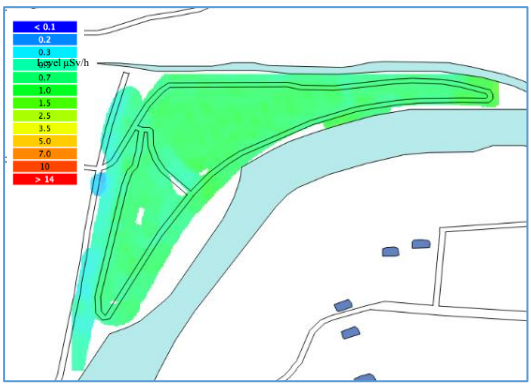


*Figure 19: Results of interpolation by IDW*

d) Walking survey in a difficult-to-return evacuation zone

We conducted a walking survey in a difficult-to-return evacuation zone in Fukushima Prefecture (Figures 20 and 21). The area where the walking survey was conducted was nearly uniform grassland. The dose rate was nearly uniform in the area, with no large deviation observed.

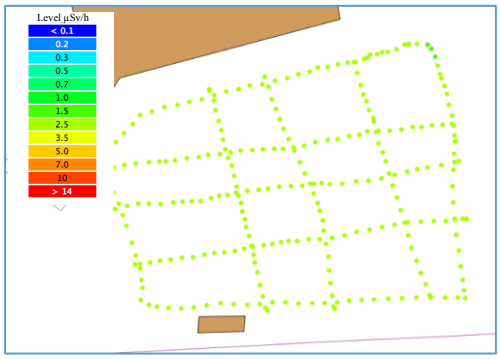


*Figure 20: Dose map*

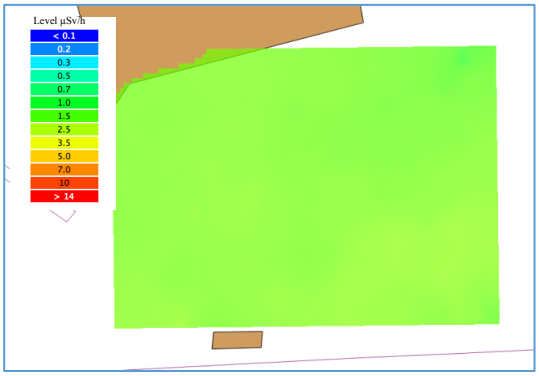


*Figure 21: Results of interpolation with IDW*

(5) Manual Production

We published a manual summarizing how to conduct walking surveys. The manual is written with a combination of pictures and text to be easily understood.

## 4.3. Summary

Results were obtained in developing walking surveys by 2015.

In terms of developed equipment, the walking survey system adopted KURAMA, which was designed by Kyoto University and has a structure suitable for a walking survey. Additionally, to analyze the obtained data or to work with other monitoring methods, such as a UAV survey, we prepared a GIS data processing system. Furthermore, by collecting data for the determination of direction characteristics and calibration constants, it has become possible to measure the dose rate in a walking survey.

We conducted walking surveys at several points and confirmed that it is possible to measure the air dose rate and to create a contour map with a GIS processing system.

We published a manual for walking surveys and made the manual available to the general public.

# 5. FIP5: Project for the study of promoting the proper treatment of waste containing radioactive materials at municipal solid-waste incinerators


## Summary

To understand changes in the migration of radiocaesium to fly ash due to changes in the combustion temperature in the municipal solid-waste (MSW) incinerator or the addition of a radiocaesium volatility accelerator or inhibitor, we conducted demonstration tests in MSW incineration facilities in operation. We also conducted coincineration tests of radiocaesium bearing used filter cloth from bag filters with MSW at operating incinerators, and leaching tests of radiocaesium in bottom ash and fly ash generated from MSW incineration facilities in Fukushima Prefecture.


## 5.1. Purpose

Incinerating MSW that contains radiocaesium dispersed in the accident at the Fukushima Daiichi Nuclear Power Plant causes radiocaesium to migrate to and concentrate in bottom ash and fly ash. Bottom and fly ash generated in this way cannot be disposed of in a landfill even if it has a radiocaesium concentration below 8000 Bq/kg, the standard set forth by law, and bottom ash and fly ash that must be stored has thus accumulated.

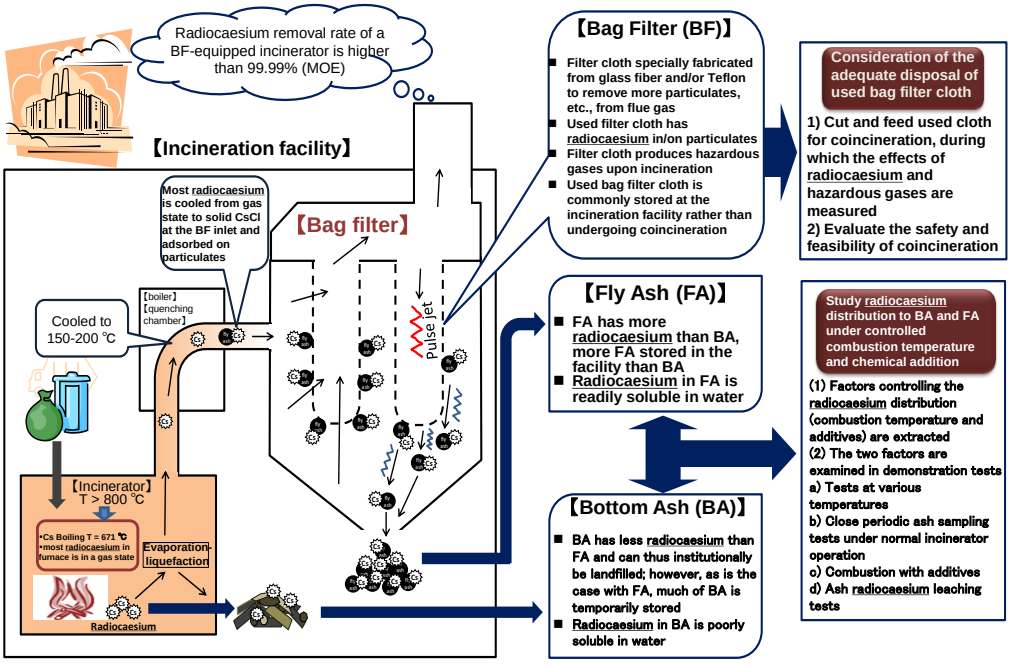


*Figure 1: Issues in the waste combustion process and test study*

Although the level of radioactivity has decreased appreciably since immediately after the accident, ash containing radioactive substances is still being generated daily by the incineration of daily MSW. Properly treating and disposing of this ash is an urgent issue (Figure 1).

We thus decided to conduct demonstration tests to confirm the effectiveness of methods that control the migration of radiocaesium to bottom ash and fly ash. After clarifying general aspects of leaching characteristics of incineration ash generated in Fukushima Prefecture, we developed technologies that remove radiocaesium from bottom ash and fly ash, and methods that make soluble radiocaesium in bottom ash and fly ash hardly soluble.

Used filter cloth of bag filters with radioactive materials attached to the cloth is also generated by incineration facilities. The proper treatment of the cloth also poses a challenge.

The coincineration of the cloth with MSW is conceivable. To confirm the feasibility of coincineration, it is necessary to understand the coincineration-induced change in the radiocaesium distribution to bottom ash and fly ash and its effect on the incineration facility and the environment when coincineration is conducted. We thus conducted coincineration demonstration tests.

## 5.2. Implementation Details

(1) Distribution of radiocaesium to bottom ash and fly ash

Radiocaesium is known to have a tendency to generally evaporate during incineration and to transfer to fly ash rather than remaining in bottom ash. The ratios of the distribution of radiocaesium to bottom ash and fly ash at incineration facilities in Fukushima Prefecture are given in Table 1. The table shows that approximately 60% of total radiocaesium is transferred to fly ash.

The literature gives five main factors that possibly govern the transfer of radiocaesium: (a) the combustion temperature, (b) the air ratio, (c) the waste composition, (d) the addition of chemicals, and (e) the particle size of ash.

Among the factors listed, (b) the air ratio (air volume) affects various system parameters, including the flue gas velocity, which possibly disturbs the combustion balance and affects proper incineration, (c) the waste composition cannot be controlled, and (e) the ash particle size is technically difficult to control. We thus focused our demonstration test on the relationships between the migration behavior of radiocaesium and (a) the combustion temperature and (d) the addition of chemicals.

*Table 1: Radiocaesium distribution to bottom ash/fly ash of MSW incineration facilities in Fukushima Prefecture*

| Facility | Capacity | Dust collection | Annual incineration (2011 fy) | Ash generation | | Radiocaesium concentration | | Radiocaesium distribution | |
|---|---|---|---|---|---|---|---|---|---|
| | | | | BA | FA | BA | FA | BA | FA |
| | t/d | | t/y | t/y | t/y | Bq/kg | | % | |
| a | 105 | BF | 16,035 | 2053 | 632 | 12,220 | 49,400 | 45 | 55 |
| b | 150 | EP | 35,612 | 4797 | 724 | 7540 | 45,500 | 52 | 48 |
| c | 80 | BF | 20,230 | 2190 | 1076 | 16,640 | 33,900 | 50 | 50 |
| d | 30 | BF | 4574 | 381 | 86 | 1706 | 12,260 | 38 | 62 |
| e | 100 | EP | 30,111 | 2912 | 737 | 3920 | 36,300 | 30 | 70 |
| f | 120 | BF | 28,964 | 4019 | 747 | 3910 | 34,900 | 38 | 62 |
| g | 40 | BF | 12,401 | 2190 | 262 | 2200 | 17,360 | 51 | 49 |
| h | 50 | BF | 837 | 93 | 41 | 3140 | 13,110 | 35 | 65 |
| i | 60 | BF | 10,181 | 1342 | 336 | 639 | 4650 | 35 | 65 |
| j | 50 | BF | 8906 | 720 | 422 | 2269 | 5690 | 40 | 60 |
| k | 90 | BF | 16,948 | 1392 | 681 | 1494 | 6640 | 31 | 69 |

Note 1 Values in this table are not corrected for the amount of water or agents added.
Note 2 Incinerators at all facilities are of the stoker furnace.
Note 3 Radiocaesium concentrations were measured in July 2011.
Note 4 Dust collection method, BF: bag filter; EP: electrostatic precipitator
Note 5 Symbols for the facility here differ from those used in the text.

a) Tests for various combustion temperatures

We obtained the cooperation of Facilities A to D in conducting our tests. All facilities were equipped with a stoker furnace.

We compared the distribution of radiocaesium to bottom ash and fly ash when the temperature at the incineration chamber exit was raised (or lowered) 50° C from the normal operating temperature with the distribution during normal operation.

To get a combustion chamber outlet temperature of 50° C higher or lower than that in normal operation, we raised or lowered the temperature of combustion air supplied to the combustion chamber (i.e., primary air) by approximately 50° C from the temperature during normal operation. The amount of combustion air (i.e., primary air) was not changed to prevent changes in the production ratio of bottom ash and fly ash due to ash blow up. Other operating conditions, such as those relating to the furnace water spray and amount of secondary air, differed between facilities.

Because the actual combustion temperature (in the combustion zone inside the furnace) cannot be measured, we used the temperature at the combustion chamber outlet measured in common at each facility as an index, and evaluated the effect of the changes in this temperature on the migration behavior of radiocaesium.

The test operation was continued for 1 day (i.e., 24 hours) under the same conditions in consideration of the time needed to stabilize the combustion state and the long retention time of bottom ash in the system.

We sampled fly ash and flue gas at least 1 hour after the establishment of the test conditions.

As for bottom ash, because of the facility-specific long time of retention inside the incinerator and ash discharger, we predetermined, for each facility, a sampling time based on the retention times estimated in a simple model calculation and a tracer test (where metal cans were thrown into the waste hopper and their arrival was observed at a planned sampling point).

As an example, Figure 2 shows sampling points for bottom ash, fly ash, and exhaust gas, and estimated retention times of bottom ash inside the system for Facility A.

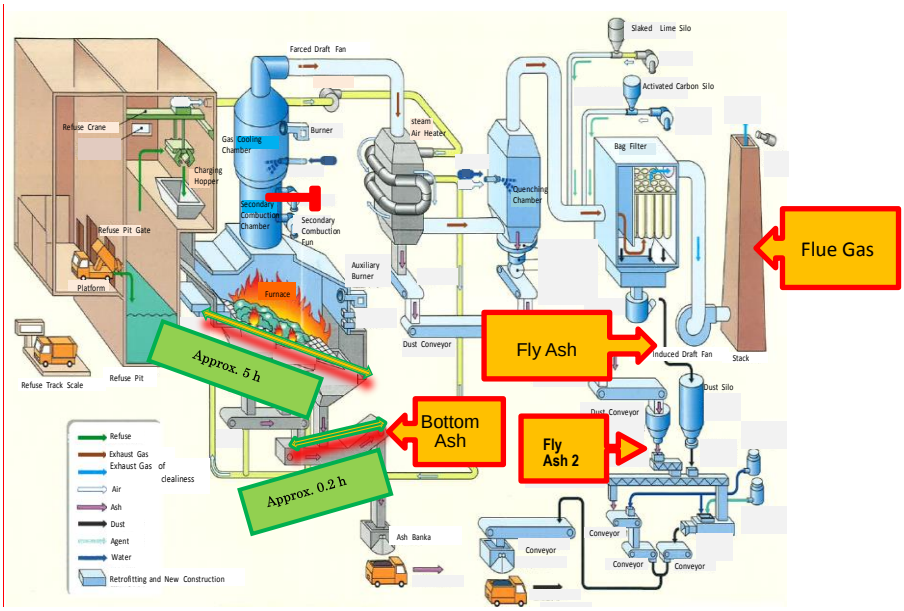


*Figure 2: Sampling Points and System Retention Time (Facility A)*

We conducted measurements and analysis as shown in Table 2 for the bottom ash, fly ash, and flue gas sampled as described above.

*Table 2: Collected samples and measurement items*

| |
|---|
| Waste Composition: Three components, composition, heating value, elemental analysis<br>Bottom Ash: Radiocaesium concentration (Note 1)<br>Cs, Na, K, Ca, Mg, Al, Si, P, Fe, ignition loss (Note 2)<br>Fly Ash: Radiocaesium concentration (Note 1)<br>Cs, Na, K, Ca, Mg, Al, Si, P, Fe<br>Flue Gas: Radiocaesium concentration (Note 3)<br>Dioxins (Note 2)<br>Note 1: 4 samples of bottom ash and fly ash were collected every hour. Four were mixed and distributed for the analysis. Radiocaesium concentration of 4 samples before mixing were also subject to NaI gamma ray spectrometer measurement.<br>Note 2: Conducted to check that there is no incomplete combustion under low temperature operation.<br>Note 3: Conducted to check that there is not increased radiocaesium under high temperature operation and operation with radiocaesium evaporation promotoion agents added |

Analytical results of the waste composition are given in Table 3 and constitute the most basic information about waste. Compositional differences are thought to define the behavior of radiocaesium in the combustion process. We cannot observe a clear relationship between the composition of waste and the area or season that the waste was generated. In regard to the lower calorific value of the waste incinerated, Facilities A and B had calorific values of 8330 to 9920 kJ/kg, while all values exceeded 10,000 kJ/kg at Facility C, which had slightly higher caloric waste in the summer. Meanwhile, although Facility D received autumn waste at the end of November, it had the lowest lower calorific value.

*Table 3: Waste composition analysis*

| Facility | | | A | | | B | | C | | D | |
|---|---|---|---|---|---|---|---|---|---|---|---|
| Collection Date (2014) | | | 6/26 | 6/27 | 10/15 | 7/9 | 7/10 | 7/29 | 7/30 | 11/25 | 11/28 |
| Apparent Specific Gravity | | (kg/m³) | 220 | 217 | 131 | 139 | 223 | 97 | 126 | 184 | 176 |
| Moisture Content | | (%) | 45.65 | 47.12 | 39.18 | 43.16 | 45.13 | 36.38 | 45.78 | 49.38 | 45.15 |
| Ash Content | | (%) | 9.72 | 6.32 | 10.16 | 8.00 | 7.36 | 5.54 | 6.14 | 8.15 | 6.86 |
| Lower Calorific Value | | (kJ/kg) | 8,460 | 9,380 | 9,920 | 8,330 | 9,420 | 12,100 | 10,130 | 7,700 | 8,620 |
| Composition of Dried Waste | Paper/Cloth | (%) | 53.0 | 38.4 | 39.4 | 59.2 | 45.4 | 56.3 | 37.5 | 39.0 | 49.7 |
| | Plastic/ synthetic resin/rubber/ leather | (%) | 22.6 | 27.1 | 18.6 | 15.5 | 21.2 | 22.7 | 32.9 | 21.4 | 24.1 |
| | Wood/bamboo/straw | (%) | 13.7 | 10.0 | 24.8 | 8.1 | 11.2 | 6.7 | 12.0 | 14.1 | 8.3 |
| | Kitchen waste | (%) | 3.7 | 14.3 | 9.5 | 13.9 | 10.4 | 9.2 | 8.4 | 14.9 | 10.0 |
| | Non-burnable | (%) | 2.3 | 2.4 | 5.1 | 0.4 | 4.6 | 0.6 | 2.5 | 4.3 | 0.7 |
| | Other (under 5 mm) | (%) | 4.7 | 7.8 | 2.6 | 2.9 | 7.2 | 4.5 | 6.7 | 6.3 | 7.2 |
| Ash Content of Dried Waste | Paper/Cloth | (%) | 5.6 | 4.4 | 5.0 | 7.7 | 2.9 | 4.9 | 4.3 | 3.7 | 4.5 |
| | Plastic/ Synthetic resin/rubber/ leather | (%) | 1.9 | 1.2 | 1.0 | 0.9 | 1.4 | 1.2 | 1.6 | 1.9 | 2.7 |
| | Wood/bamboo/straw | (%) | 4.7 | 1.1 | 3.1 | 1.6 | 0.4 | 0.4 | 0.7 | 0.8 | 0.9 |
| | Kitchen waste | (%) | 0.7 | 1.0 | 1.1 | 2.5 | 1.5 | 0.6 | 0.6 | 3.1 | 1.7 |
| | Non-burnable | (%) | 2.3 | 2.4 | 5.1 | 0.4 | 4.6 | 0.6 | 2.5 | 4.3 | 0.7 |
| | Other (under 5 mm) | (%) | 2.7 | 1.9 | 1.3 | 1.1 | 2.6 | 1.0 | 1.6 | 2.3 | 2.0 |
| | Total | (%) | 17.9 | 12.0 | 16.6 | 14.2 | 13.4 | 8.7 | 11.3 | 16.1 | 12.5 |
| Elemental Composition | Carbon | (%) | 40.36 | 49.98 | 47.11 | 44.15 | 48.27 | 50.91 | 54.47 | 44.37 | 46.90 |
| | Hydrogen | (%) | 6.36 | 8.10 | 7.19 | 6.49 | 7.19 | 8.23 | 9.30 | 7.07 | 7.10 |
| | Nitrogen | (%) | 0.71 | 0.81 | 1.16 | 1.18 | 1.48 | 0.56 | 0.66 | 0.97 | 0.61 |
| | Sulfur | (%) | 0.08 | 0.07 | 0.00 | 0.07 | 0.08 | 0.06 | 0.07 | 0.06 | 0.07 |
| | Chlorine | (%) | 0.31 | 0.16 | 0.81 | 0.15 | 0.57 | 0.42 | 0.42 | 0.21 | 0.21 |
| | Oxygen | (%) | 36.20 | 31.07 | 31.48 | 34.20 | 33.19 | 31.68 | 26.00 | 34.97 | 33.17 |

b) Continuous sampling tests

As a next step, we dared not to manage operating conditions but instead implemented demonstration tests to understand the relationship between the combustion temperature and behavior of migration (distribution) of radiocaesium to bottom ash and fly ash during normal operation.

We sampled bottom ash and fly ash sampling every 2 hours for 5 days continuously at Facilities B and F. The concentration of radiocaesium of each sample was measured with a NaI (Tl) scintillation spectrometer (hereinafter referred to as the NaI measurement). We also measured the concentration of radiocaesium using a germanium semiconductor detector (hereinafter referred to as the Ge measurement).

The first four samples taken each day were mixed together and then divided and distributed for Ge measurement and elemental (Cs, Na, K, Ca, Mg, Al, Si, P, and Fe) analysis. With the data acquired, the relationship between the combustion temperature during normal operation and migration behavior (distribution to bottom ash/fly ash) of radiocaesium was examined.

The methods used to decide the sampling points and timings were those employed in subsection (1)-a).

c) Tests that confirm the effects of a radiocaesium evaporation accelerator and inhibitor

We conducted tests adding hydrated lime ($Ca(OH)_2$), which is expected to promote the evaporation of radiocaesium, and tests adding bentonite (clay), which is expected to inhibit the evaporation of radiocaesium.

We first conducted additive tests of hydrated lime and bentonite at Facility A. We introduced hydrated lime equal to 5.5w% or bentonite equal to 2.2w% of the waste. The materials were sprayed on the surface of each crane grasp of waste thrown into the hopper.

The first test revealed that hydrated lime had an appreciable effect on the concentration of radiocaesium, and we subsequently conducted supplementary tests in which we added hydrated lime. In one test, hydrated lime was added at ratios of 2.6w% and 5.5w% at the same Facility A to check the reproducibility of the effect of hydrated lime. To confirm whether this phenomenon was facility specific, another test was conducted at Facility D with hydrated lime added at a ratio of 2.2w%.

(2) Proper-treatment test of the used filter cloth of a bag filter

We conducted two coincineration tests of filter cloths with MSW. One was conducted at Facility B, whose filter cloths are made of glass fiber, and the other at Facility E, whose filter cloths are made of Teflon. Both facilities are equipped with a stoker furnace. Test conditions were combinations of different filter cloth throw-in ratios and intervals (Table 4).

*Table 4: Details of the used bag filter cloth coincineration test*

| Facility name | | | B (60 t/furnace·day) | | | E (75 t/furnace·day) | | |
|---|---|---|---|---|---|---|---|---|
| Filter cloth material | | | Glass fiber | | | Teflon® (polytetrafluoroethylene, PTFE) | | |
| Run | | | RUN 1 | RUN 2 | RUN 3 | RUN 1 | RUN 2 | RUN 3 |
| Coincineration ratio | | | Normal operation | 0.2% | 0.4% | Normal operation | 0.03% | |
| Filter cloth input amount | | | | 6.4 kg/H | 12.8 kg/H | | 0.90 kg/H | |
| Input amount and time interval, time continued | | | | (1.5/0.5 H), 6 h | 3/0.5 H, 6 H | | 0.5/1 H, 6 H | 1.5/3H, 6 H |
| Measurement item | Used filter cloth | Radiocaesium | ○ | | | ○ | | |
| | Flue gas | Radiocaesium | ○ | ○ | ○ | ○ | – | ○ |
| | | Hydrogen chloride | – | ○ | ○ | – | ○ | ○ |
| | | Sulfur oxide | – | ○ | ○ | – | ○ | ○ |
| | | Nitrogen oxide | – | ○ | ○ | – | ○ | ○ |
| | | Dioxins (*2) | – | – | ○ | – | – | ○ |
| | | Fluorine compounds | – | – | – | ○ | ○ (four times) | ○ (four times) |
| | Bottom ash | Radiocaesium (*1) | ○ | ○ | ○ | ○ | ○ | ○ |
| | | Ignition loss (*2) | – | – | ○ | – | – | ○ |
| | Fly ash | Radiocaesium (*1) | ○ | ○ | ○ | ○ | ○ | ○ |
| *1) Radiocaesium samples were collected once per hour for NaI measurement, for a total of five collections, four of which were mixed into one sample and then divided for Ge measurement.<br>*2) Conducted in the RUN under the most severe conditions. | | | There were two cases of the coincineration ratio (average 0.20% and maximum of 0.40%) based on questionnaire survey results of facilities that had actually conducted coincineration before.<br>Filter cloth dimensions: 164 mm φ × 5250 mmL.<br>Weight was the manufacturer's standard value: 2.38 kg each calculated from a density of 880 g/m$^2$.<br>Radiocaesium concentration of the filter cloth subject to coincineration: 600 Bq/kg. | | | The coincineration ratio was set at 0.03%, referencing "Seiso Giho No. 8 2008 Tokyo 23 Special District Authority".<br>Filter cloth dimensions: 140 mm φ × 6000 mmL.<br>Weight was the manufacturer's standard value: 1.71 kg each calculated from a density of 650 g/m$^2$, but the measured value at the facility was 2.0 kg each.<br>Radiocaesium concentration of the filter cloth subject to coincineration: 1260 Bq/kg. | | |

Regarding the effects of coincineration on the migration behavior of radiocaesium due to fly ash that contains radiocaesium adhering to the filter cloth, the effect of waste with glass fiber that is difficult to combust on the combustion state, and the increase in concentration of fluorine compounds due to the combustion of Teflon, we collected and analyzed bottom ash, fly ash, and flue gas before and during the test, or collected data of measurements made by the facility. For these items, we then compared the data obtained before inputting the filter cloth and during the test and surveyed the effects. Sampling points and times were set according to the methods described in subsection (1)-a).

(3) Understanding radiocaesium leaching characteristics of bottom ash and fly ash

We conducted leaching tests for 15 pairs of bottom ash and fly ash sampled from six incineration facilities, Facilities A to F. The tests were based on the "JIS K0058-1 'As is' Stir Test" method of placing 250 g of a sample as is into a container, adding 10 times the amount (L/kg) of pure water, and then stirring the upper liquid portion with a propeller.

## 5.3. Results and Discussion

(1) Distribution of radiocaesium between bottom ash and fly ash

a) Tests for different combustion temperatures

Data on the migration and distribution of radiocaesium gained from tests are given in Table 5.

*Table 5: Combustion temperature and migration of radiocaesium for each facility and each test*

| Facility | Test date | Test | Primary air temp | Combustion chamber outlet temp | Radiocaesium concentration Bq/kg (measurement value) | | Radiocaesium concentration Bq/kg (corrected value (*1)) | | Distribution ratio % of radiocaesium to fly ash | Fly ash/bottom ash radiocaesium concentration ratio (*2) |
|---|---|---|---|---|---|---|---|---|---|---|
| | | | ° C | | Bottom ash | Fly ash | Bottom ash | Fly ash | | |
| A | 6/23 | Standard 1 | 125 | 904 | 1580 | 8300 | 1900 | 13000 | 60 | 6.8 |
| | 6/24 | Standard 2 | 121 | 912 | 1750 | 10300 | 2100 | 16000 | 63 | 7.6 |
| | 6/26 | High temp 1 | 183 | 964 | 2020 | 10800 | 2500 | 17000 | 61 | 6.8 |
| | 6/27 | High temp 2 | 189 | 950 | 1460 | 13500 | 1900 | 21000 | 72 | 11.1 |
| | 7/2 | Hydrated lime 2.4% | 119 | 923 | 840 | 14800 | 1100 | 23000 | 84 | 20.9 |
| | 7/3 | Bentonite 2.2% | 123 | 940 | 1990 | 14600 | 2400 | 23000 | 69 | 9.6 |
| A Add. | 10/14 | Standard | 121 | 904 | 1260 | 14500 | 1400 | 20000 | 76 | 14.3 |
| | 10/16 | Hydrated lime 2.6% | 116 | 891 | 920 | 15700 | 1200 | 22000 | 83 | 18.3 |
| | 10/17 | Hydrated lime 5.5% | 116 | 904 | 540 | 10400 | 650 | 15000 | 84 | 23.1 |
| B | 7/8 | Low temp 1 | 101 | 855 | 1020 | 5700 | 1200 | 6800 | 68 | 5.7 |
| | 7/9 | Low temp 2 | 103 | 842 | 900 | 4600 | 980 | 5500 | 67 | 5.6 |
| | 7/10 | High temp 2 | 200 | 946 | 940 | 5100 | 1000 | 6100 | 68 | 6.1 |
| | 7/11 | High temp 2 | 194 | 956 | 590 | 4700 | 630 | 5600 | 76 | 8.9 |
| C | 7/28 | Standard 1 | 52 | 933 | 930 | 7800 | 1100 | 12000 | 71 | 10.9 |
| | 7/29 | High temp 1 | 100 | 931 | 1110 | 6400 | 1300 | | 64 | 7.6 |
| | 7/30 | High temp 2 | 100 | 924 | 1740 | 9600 | 1800 | 15000 | 63 | 8.3 |
| | 7/31 | Standard 2 | 52 | 937 | 1490 | 9500 | 1700 | 15000 | 64 | 8.8 |
| D | 11/25 | Standard 1 | 178 | 880 | 480 | 1590 | 430 | 2900 | 54 | 6.7 |
| | 11/26 | High temp 1 | 129 | 867 | 480 | 1450 | 430 | 2600 | 52 | 6.0 |
| | 11/27 | High temp 2 | 134 | 873 | 453 | 1470 | 400 | 2600 | 54 | 6.5 |
| | 11/28 | Standard 2 | 177 | 883 | 530 | 1250 | 470 | 2200 | 46 | 4.7 |
| | 11/29 | hydrated lime 2.2% | 178 | 893 | 410 | 1280 | 360 | 2300 | 53 | 6.4 |

(*1) Measured values were corrected for flue gas treatment agents and water added during the process.

(*2) Corrected values were used.

The tests were conducted in four facilities, but we were unable to obtain a combustion chamber outlet temperature higher than that of standard operation during high-temperature operation at Facility C. Additionally, at Facility D, we were unable to obtain a combustion chamber outlet temperature lower than that of standard operation in low-temperature operation.

Facilities A and B ran for two days at high combustion temperature through high-temperature operation. A high rate of radiocaesium distribution to fly ash was achieved on the second day. Linear approximations with exclusion of data of the first day give an increased radiocaesium distribution rate of 2.6% (Facility A) and 0.8% (Facility B) per ~10 °C increase in the incineration temperature (Figures 3 and 4).

To see the variation in temperature and the migration status of radiocaesium before and

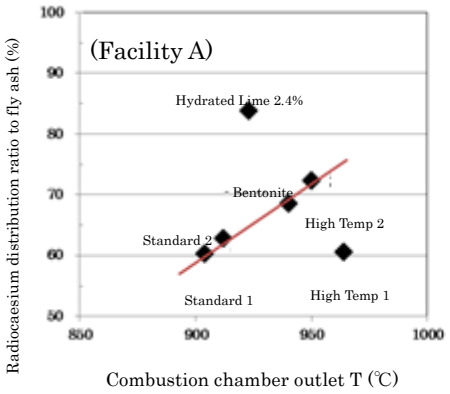


*Figure 3: Rate of distribution of radiocaesium to fly ash versus the combustion chamber outlet temperature (Facility A)*

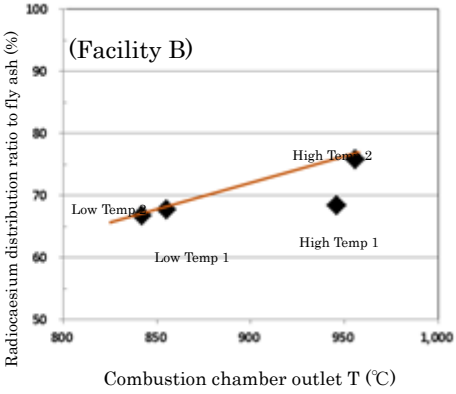


*Figure 4: Rate of distribution of radiocaesium to fly ash versus the combustion chamber outlet temperature (Facility B)*

after changing the combustion temperature conditions from standard to high-temperature operation, we sampled bottom ash and fly ash every 2 hours for 2 days during the test at Facility B, and conducted a NaI measurement. Results confirmed that with the change in operation mode from low-temperature operation to high-temperature operation, the combustion chamber outlet temperature increased approximately 100 °C, from 850 to 950 °C, and the fly ash/bottom ash ratio of the radiocaesium concentration increased along with the increasing temperature (Figure 5).

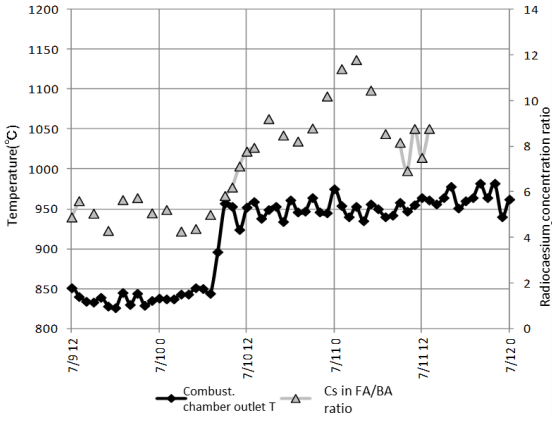


*Figure 5: Combustion chamber outlet temperature and radiocaesium concentration ratio (Facility B)*

b) Continuous sampling test

Figures 6 (Facility B) and 7 (Facility F) show the combustion chamber outlet temperature, NaI-measured radiocaesium concentration in bottom ash and fly ash, ratio of the radiocaesium distribution to fly ash based on NaI measurement, and ratio of the radiocaesium distribution ratio to fly ash based on Ge measurement.

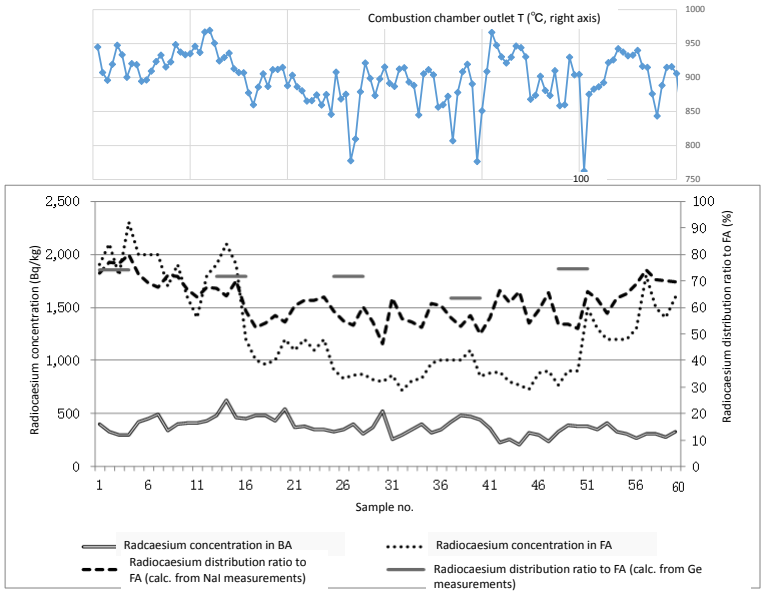


*Figure 6: Radiocaesium concentration in bottom ash and fly ash from NaI measurement, radiocaesium distribution ratio from both NaI and Ge data, and combustion chamber outlet temperature (dry basis, Facility B)*

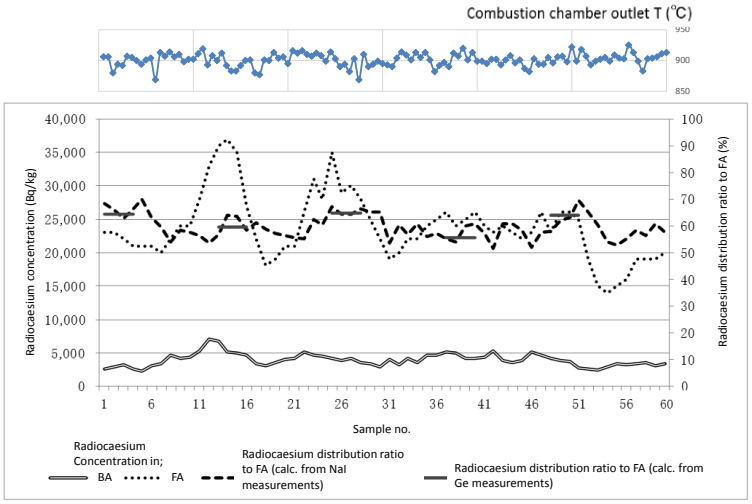


*Figure 7: Radiocaesium concentration in bottom ash and fly ash from NaI measurement, radiocaesium distribution ratio from both NaI and Ge data, and combustion chamber outlet temperature (dry basis, Facility F)*

It is difficult to see a clear relationship between the combustion chamber outlet temperature and the distribution of radiocaesium to fly ash.

Looking at the plots of the temperature and the ratio of the radiocaesium distribution to fly ash based on NaI measurement data (Figures 8 and 9), the rising combustion chamber outlet temperature at Facility B was accompanied by a rising ratio of the radiocaesium distribution to fly ash. Sudden drops in temperature may correspond to the inputs of sewage sludge, and it should be noted that the waste composition has also largely changed. The range of variation in the outlet temperature of the combustion chamber of Facility F was small, and no clear proportional relationship between the radiocaesium distribution ratio and combustion chamber outlet temperature was observed.

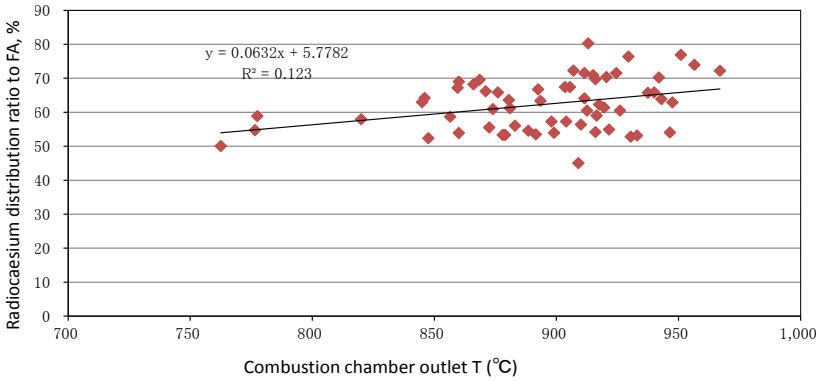


*Figure 8: Combustion chamber outlet temperature versus the ratio of the radiocaesium distribution to fly ash (Facility B), with the radiocaesium concentration obtained by NaI measurement*

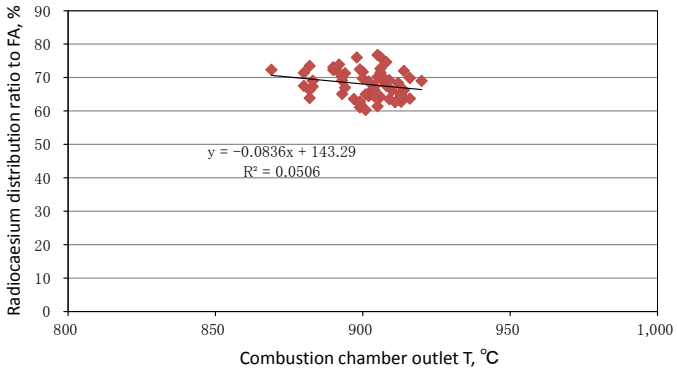


*Figure 9: Combustion chamber outlet temperature versus the ratio of the radiocaesium distribution to fly ash (Facility B), with the radiocaesium concentration obtained by NaI measurement*

The data taken continuously over 5 days for Facility F show a weak positive correlation between the ratio of the radiocaesium distribution to fly ash and the waste basicity (Figure 10), but no correlation with the chlorine content can be observed (Figure 11). The basicity of the waste was calculated from the chemical compositions of bottom ash and fly ash.

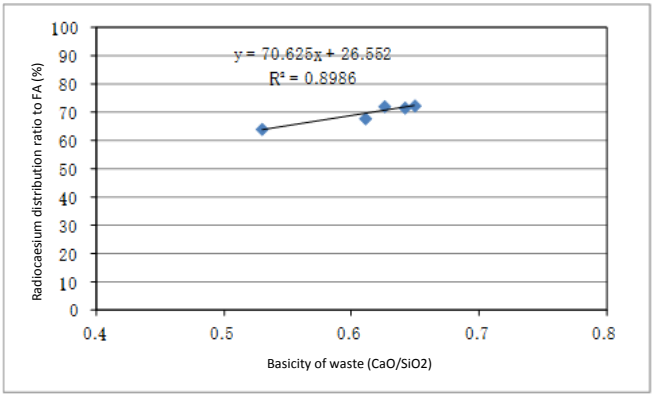


*Figure 10: Basicity of the waste calculated from the chemical composition of bottom ash and fly ash versus the ratio of the radiocaesium distribution to fly ash (Facility F)*

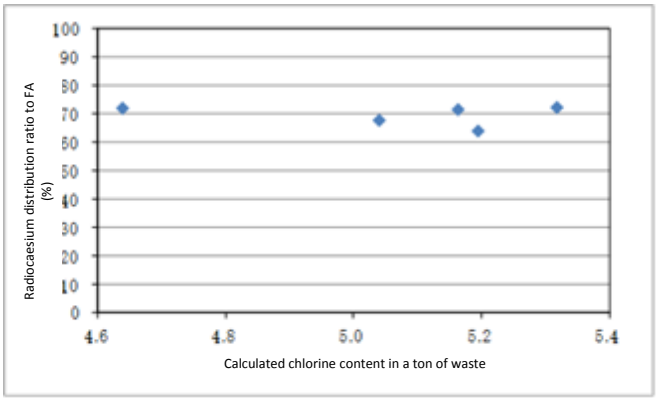


*Figure 11: Chlorine content in the waste calculated from the chemical composition of bottom ash and fly ash versus the ratio of the radiocaesium distribution to fly ash (Facility F)*

c) Tests that confirm the effects of a radiocaesium evaporation accelerator and inhibitor

An appreciable rise in the ratio of the radiocaesium distribution to fly ash (a 9.3% rise in the distribution ratio per 1% additive rate) was observed in the first hydrated-lime additive test at Facility A, but the inhibiting effect of bentonite was not confirmed (Figure 3).

We conducted additional tests to confirm the effects of adding hydrated lime, and a certain effect was confirmed at Facility A but it was not as great as in the first test. It was confirmed that there was no effect at Facility D (Figure 12).

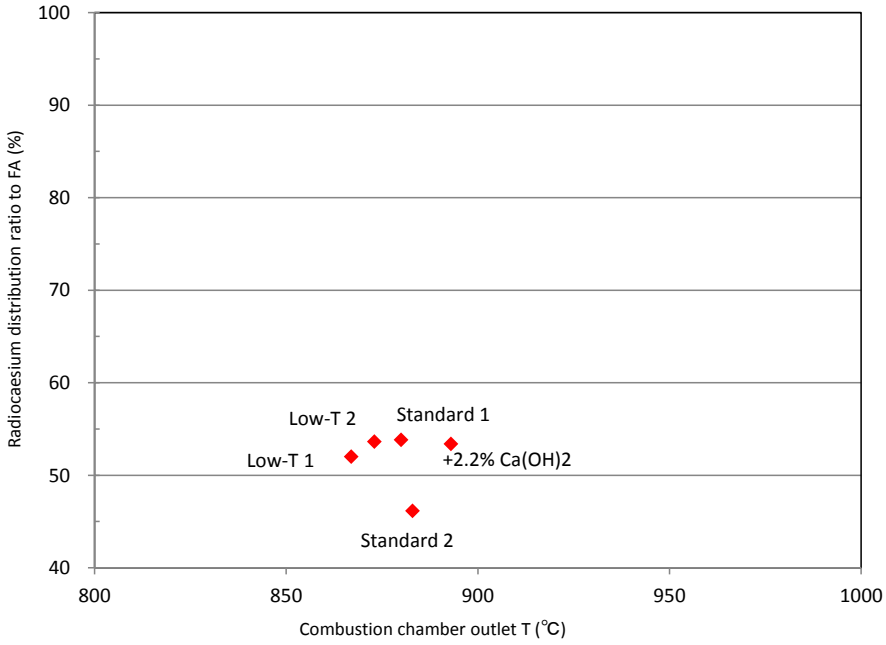


*Figure 12: Effect of adding hydrated lime on the ratio of the radiocaesium distribution to fly ash (Facility D)*

According to a literature survey, higher basicity of the incinerated matter should accelerate the evaporation of radiocaesium. Basicity of the waste calculated from the chemical analysis of bottom ash and fly ash conducted at Facilities A to D is given in Table 6. The table shows that the basicity of waste at Facility A was lower than that at other facilities. It is probable that the obvious effect observed at Facility A was due to adding the basicity-increasing agent, hydrated lime, to low-basicity waste. Yet in the case of Facility D, it is possible that the basicity-increasing agent was added to waste whose basicity was high to a certain degree, and the hydrated lime thus did not promote the evaporation of radiocaesium.

In this demonstration test, we had tight operating conditions that differ from the conditions of usual operation, and it was thought that the operations increased the radiocaesium concentration in flue gas. We therefore conducted measurements of flue gas and dioxins. As a result, no radiocaesium was found in the flue gas. Furthermore, the dioxin concentration in flue gas and ignition loss values of bottom ash met the criteria of relevant regulations.

*Table 6: Basicity of waste calculated from the chemical compositions of bottom ash and fly ash*

| Facility | A | | | | | | B | | C | | D | | |
|---|---|---|---|---|---|---|---|---|---|---|---|---|---|
| Ash sampling date (2014) | 6/23 | 6/26 | 7/2 | 10/14 | 10/16 | 10/17 | 7/8 | 7/10 | 7/28 | 7/29 | 11/25 | 11/26 | 11/29 |
| Hydrated lime added (w%) | - | - | 2.4 | - | 2.6 | 5.5 | - | - | - | - | - | - | 2.2 |
| CaO/SiO2 | 0.44 | 0.55 | 1.03 | 0.65 | 1.02 | 1.42 | 0.82 | 1.11 | 0.96 | 0.62 | 0.67 | 0.75 | 1.42 |
| | 0.49 | | | | | | 0.95 | | 0.77 | | 0.71 | | |
| (CaO+MgO+Al2O3) /SiO2 | 0.81 | 0.97 | 1.43 | 1.07 | 1.46 | 1.89 | 1.38 | 1.79 | 1.58 | 1.13 | 1.11 | 1.22 | 1.89 |
| | 0.88 | | | | | | 1.56 | | 1.33 | | 1.16 | | |
| Radiocaesium distribution ratio to FA (%) | 61 | 61 | 84 | 76 | 83 | 84 | 68 | 68 | 71 | 64 | 54 | 52 | 53 |

*Calculation of basicity for the days on which hydrated lime was added. We used the average of analyzed values of the dates 6/26 and 6/23 for 7/2, the analyzed values of the date 10/14 for 10/16 and 10/17, and the average of analyzed values of the dates 11/25 and 11/26 for 11/29.*

(2) Proper-treatment test of the used filter cloth of a bag filter

Coincineration of used filter cloth with MSW was confirmed safe and feasible under the proper management of the coincineration ratio.

Regarding many measurements that we made, used filter cloth coincineration did not affect the measurements but increased the concentration of radiocaesium in ash (Table 7). This increase was observed at Facility B and no increase was observed at Facility E. The increase is thought to be caused by a change in the radiocaesium concentration in MSW coincinerated rather than the input of used filter cloth. This is supported by two pieces of evidence. First, the increase was higher than the value calculated from the radiocaesium concentration of the input filter cloth. Second, the increased values remained within the range of variation of the measurements that the facility made in 2015. No radiocaesium was detected in flue gas and no effects of coincineration on flue gas were confirmed. Table 8 presents the case for Facility E.

*Table 7: Radiocaesium concentration in bottom ash and fly ash*

| Facility | | B | | | E | | |
|---|---|---|---|---|---|---|---|
| Test RUN No. | | RUN 1 | RUN 2 | RUN 3 | RUN 1 | RUN 2 | RUN 3 |
| Used filter cloths input | | - | 1.5/0.5H | 3.0/0.5H | - | 0.5/1.0H | 1.5/3.0H |
| Radiocaesium concentration (Bq/kg) | Bottom ash | 318 | 400 | 800 | 266 | 157 | 105 |
| | Fly ash | 2400 | 3260 | 3640 | 1400 | 1210 | 1220 |

*Table 8: Radiocaesium in flue gas*

| Flue gas from No.1 furnace of Facility E | | | | | |
|---|---|---|---|---|---|
| Sampling point | | | BF outlet | | |
| Sampling date (2015) | | | 10.26 | 10.27 | 10.28 |
| RUN No. and used filter cloth input | | | RUN 1 | RUN 2 | RUN 3 |
| | | | – | 0.5/H | 1.5/3H |
| Radiocaesium concentration ($Bq/m^3N$) | Filter | Cs-134 | <0.3 | <0.3 | <0.3 |
| | | Cs-137 | <0.3 | <0.3 | <0.3 |
| | Drain | Cs-134 | <0.3 | <0.3 | <0.3 |
| | | Cs-137 | <0.3 | <0.3 | <0.3 |
| Wet flue gas flow | | ($m^3N/h$) | 37,600 | 38,500 | 35,300 |
| Dry flue gas flow | | (m3N/h) | 26,100 | 27,100 | 25,600 |
| Moisture content | | (%) | 30.2 | 29.6 | 27.1 |
| Gas composition | CO2 | (%) | 5.6 | 6.7 | 6.3 |
| | O2 | (%) | 14.7 | 13.5 | 13.8 |
| | CO | (%) | <0.01 | <0.01 | <0.01 |
| | N2 | (%) | 79.7 | 79.8 | 79.9 |

There were no changes in the ignition loss of bottom ash, harmful acidic substances, and dioxins in flue gas at either facility. These items are conceivably affected when combustion conditions deteriorate (Table 9).

*Table 9: Harmful acidic substances and dioxins in flue gas, and ignition loss of bottom ash*

| Facility | | | Facility B | | | Facility E | | |
|---|---|---|---|---|---|---|---|---|
| RUN No. | | | RUN 2 | RUN 3 | Past figure | RUN 2 | RUN 3 | Past figure |
| Flue gas | SOx | ($m^3N/h$) | <5 | <5 | <10 (2015) | <5 | <5 | <3.5～80 (2015) |
| | NOx | (ppm) | 140 | 160 | 140～150 (2015) | 150 | 170 | 99～180 (2015) |
| | HCl | ($mg/m^3N$) | <10 | <10 | 27～32 (2015) | 120 | 150 | <5～310 (2015) |
| | Dioxins | (ng-TEQ /$m^3N$) | - | 0.010 | 0.046～0.072 (2015) | - | 0.0028 | 0.060～0.099 (2015) |
| Bottom ash | Ignition loss | (%) | - | 5.1 | 5.0～8.1 (2014) | - | 5.1 | 1.3～6.2 (2014) |

(3) Understanding radiocaesium leaching characteristics of bottom ash and fly ash

To understand the general nature of radiocaesium leaching from bottom ash and fly ash, we conducted leaching tests for the ash from six MSW incineration facilities in Fukushima Prefecture. Result shows that leaching from bottom ash was limited (less than 1.4% to 16%), as it is generally considered to be, but we also confirmed that sometimes there was leaching at a very high ratio (47% to 83%) from fly ash (Tables 10-1 and 10-2). The results widely vary. A pair of ash samples from Facility D was the most interesting, having the lowest leaching rate of 47% for fly ash and the highest leaching rate of 16% for bottom ash.

Fly ash referred to here was raw ash collected using a bag filter, with no treatment, such as the addition of chelating agents, conducted.

*Table 10-1: Radiocaesium leaching test results (1)*

| Facility | | A | | | | C | | B | | | | | | | | | |
|---|---|---|---|---|---|---|---|---|---|---|---|---|---|---|---|---|---|
| Sampling date | | 2014 | | | | | | 2015 | | | | | | | | | |
| | | 6.23 | | 7.2 | | 7.28 | | 9.7 | | 9.8 | | 9.9 | | 9.10 | | 9.11 | |
| Sample type | | BA | FA | BA | FA | BA | FA | BA | FA | BA | FA | BA | FA | BA | FA | BA | FA |
| Radiocaesium concentration in solid (Bq/kg) | Cs-134 | 400 | 2100 | 300 | 3900 | 300 | 1700 | 45 | 380 | 43 | 320 | 25 | 280 | 65 | 250 | 24 | 190 |
| | Cs-137 | 1400 | 6100 | 760 | 11000 | 790 | 5500 | 220 | 1600 | 230 | 1500 | 180 | 1100 | 230 | 1100 | 130 | 960 |
| | Total | 1800 | 8200 | 1060 | 14900 | 1090 | 7200 | 265 | 1980 | 273 | 1820 | 205 | 1380 | 295 | 1350 | 154 | 1150 |
| 【Leaching test】 Radiocaesium concentration in liquid (Bq/L) | Cs-134 | 0.1 | 130 | 0.1 | 230 | 0.1 | 130 | 0.1 | 31 | 0.1 | 28 | 0.1 | 20 | 0.1 | 15 | 0.1 | 18 |
| | Cs-137 | 1 | 360 | 3 | 670 | 2 | 380 | 1 | 130 | 0.1 | 110 | 0.1 | 94 | 0.1 | 70 | 0.1 | 77 |
| | Total | 1 | 490 | 3 | 900 | 2 | 510 | 1 | 161 | 0.2 | 138 | 0.2 | 114 | 0.2 | 85 | 0.2 | 95 |
| Leaching rate (%) | | 0.6 | 59 | 3.6 | 61 | 2.2 | 65 | 3.8 | 81 | 0 | 76 | 0 | 83 | 0 | 63 | 0 | 83 |

*Table 10-2: Radiocaesium leaching test results (2)*

| Facility | | D | | E | | F | | | | | | | | | |
|---|---|---|---|---|---|---|---|---|---|---|---|---|---|---|---|
| Sampling date | | 2014 | | 2015 | | | | | | | | | | | |
| | | 11.25 | | 10.26 | | 10.13 | 10.12 | 10.14 | 10.13 | 10.15 | 10.14 | 10.16 | 10.15 | 10.17 | 10.16 |
| Ash type | | BA | FA | BA | FA | BA | FA | BA | FA | BA | FA | BA | FA | BA | FA |
| Radiocaesium concentration in solid(Bq/kg) | Cs-134 | 92 | 390 | 56 | 300 | 550 | 4100 | 1000 | 6300 | 700 | 5500 | 930 | 4700 | 580 | 4300 |
| | Cs-137 | 350 | 1100 | 210 | 1100 | 2300 | 17000 | 4500 | 27000 | 3100 | 23000 | 3900 | 20000 | 2500 | 18000 |
| | Total | 442 | 1490 | 266 | 1400 | 2850 | 21100 | 5500 | 33300 | 3800 | 28500 | 4830 | 24700 | 3080 | 22300 |
| 【Leaching test】 Radiocaesium concentration in liquid (Bq/L) | Cs-134 | 2 | 16 | 0.1 | 22 | 3 | 290 | 3 | 350 | 2 | 330 | 1 | 310 | 2 | 300 |
| | Cs-137 | 5 | 54 | 0.1 | 92 | 12 | 1200 | 11 | 1500 | 8 | 1400 | 6 | 1300 | 10 | 1300 |
| | Total | 7 | 70 | 0.2 | 114 | 15 | 1490 | 14 | 1850 | 10 | 1730 | 7 | 1610 | 12 | 1,600 |
| Leaching rate (%) | | 16 | 47 | 0 | 81 | 5 | 71 | 3 | 56 | 3 | 61 | 1 | 65 | 4 | 72 |

Test results thus far obtained are summarized in Table 11.

*Table 11: Summary of test results*

| Tests conducted | | Facilities used | Results obtained |
|---|---|---|---|
| (1) Distribution of radiocaesium between bottom ash/fly ash | (1)-a Tests for different combustion temperatures | A, B, C, D | Tests were conducted at four facilities, but there were cases that a facility could not be operated at the expected combustion temperature. In cases that a facility was operated at high combustion temperature, there was an increased distribution rate of radiocaesium to fly ash on the second day of operation. (When the combustion temperature increased by about 10° , the distribution ratio increased by 2.6% and 0.8% at Facilities A and B, respectively.) |
| | (1)-b Continuous sampling test | B, F | No clear relationship was seen between the combustion temperature and migration behavior of radiocaesium (distribution to bottom ash/fly ash) during normal operation. |
| | (1)-c Tests that confirm the effects of radiocaesium evaporation accelerator and inhibitor | A, D | In the first test, as a result of spraying hydrated lime (Ca(OH)2) powder as an evaporation promotion agent on waste, there was an appreciable increase in the ratio of the distribution of radiocaesium to fly ash (9.2% increase in the distribution ratio per 1% additive rate), but no inhibiting effect was seen with the addition of bentonite.<br>We conducted additional tests to confirm the reproducibility and facility dependence of the radiocaesium evaporation promotion effect of hydrated lime, and although certain evaporation effects were seen, effects as great as those observed in the first test could not be confirmed. |
| (2) Proper-treatment test of used filter cloth of bag filters | | B, E | With regard to the coincineration of radiocaesium adhering to used filter cloth with MSW, we confirmed that coincineration can be a safe and proper measure if the coincineration ratio is properly managed. |
| (3) Understanding radiocaesium leaching characteristics of bottom ash and fly ash | | A, B, C, D, E, F | We conducted tests on the leaching of radiocaesium from bottom ash and fly ash generated at six MSW incineration facilities in Fukushima Prefecture, and although the leaching rate from bottom ash was limited as it is generally believed to be (from less than 1.4% to 15%), we confirmed leaching from fly ash at a very high rate (47% to 83%). |